General Disclaimer

One or more of the Following Statements may affect this Document

- This document has been reproduced from the best copy furnished by the organizational source. It is being released in the interest of making available as much information as possible.

- This document may contain data, which exceeds the sheet parameters. It was furnished in this condition by the organizational source and is the best copy available.

- This document may contain tone-on-tone or color graphs, charts and/or pictures, which have been reproduced in black and white.

- This document is paginated as submitted by the original source.

- Portions of this document are not fully legible due to the historical nature of some of the material. However, it is the best reproduction available from the original submission.

X-733-70-119
PREPRINT

NASA TM X-63918

PROPOSAL FOR ADVANCED LASER PROPAGATION EXPERIMENTS BETWEEN STABILIZED SYNCHRONOUS SATELLITES AND GROUND STATIONS, AT VISIBLE AND NEAR-INFRARED WAVELENGTHS

ERWIN HIRSCHMANN

APRIL 1970

GODDARD SPACE FLIGHT CENTER
GREENBELT, MARYLAND

X-733-70-119
PREPRINT

PROPOSAL FOR ADVANCED LASER PROPAGATION EXPERIMENTS BETWEEN STABILIZED SYNCHRONOUS SATELLITES AND GROUND STATIONS, AT VISIBLE AND NEAR-INFRARED WAVELENGTHS

Erwin Hirschmann

April 1970

GODDARD SPACE FLIGHT CENTER
Greenbelt, Maryland

X-733-70-119
PREPRINT

PROPOSAL FOR ADVANCED LASER PROPAGATION EXPERIMENTS BETWEEN STABILIZED SYNCHRONOUS SATELLITES AND GROUND STATIONS, AT VISIBLE AND NEAR-INFRARED WAVELENGTHS

Erwin Hirschmann

April 1970

GODDARD SPACE FLIGHT CENTER
Greenbelt, Maryland

ABSTRACT

This report discusses proposed laser experiments which are to be flown on board synchronous satellites. Wavelengths of 1.06 micron (near-infrared) and 0.53 micron (optical) will be used in these experiments, which will consist of measurements of the laser propagation characteristics from ground-to-spacecraft, and measurements of the spacecraft range. Laser transmitters carried in the satellite may later permit measurements of the spacecraft-to-ground propagation characteristics.

Laser transmitters and receivers are discussed, and attenuation of the signal by various meteorological phenomena is considered.

ACKNOWLEDGMENT

The author is indebted to Mr. Michael A. Galli for his assistance.

PREFACE

Electro-optical or laser (Light Amplification by Stimulated Emission of Radiation) systems are potentially capable of fulfilling the needs associated with deep space communications and wide-band, high-rate earth/space data links for the mass transfer of information. Accordingly, NASA long-range objectives include the study and development of advanced communication systems that operate in the optical region of the spectrum. In addition to development of these systems, earth/space type experiments are needed to provide statistics to enable practical assessment of the technology and to define performance requirements for useful applications. At present, some experiments are approved and are being implemented for flight on board Application Technology Satellites. These experiments operate at the long optical wavelength region (10.6 micron). Short wavelength experiments must also be proposed and implemented so as to provide NASA the ultimate choice of the "best" type of laser communication system for specific applications. This document is an attempt, as a result of a study,* to propose short wavelength experiments which could be more fully defined and implemented for space flight.

No attempt is made here to consider spacecraft power, size, weight, etc. constraints, since the proposal is not directed to any specific mission. Instead, this document, written in terms of a proposal, is to depict a realistic experiment concept that NASA could implement, or use as guide, to define others. The content of this proposal is also indicative of the state-of-the-art.

From these or similar short wavelength experiments, data can be obtained to enable trade-off comparisons to be made with the longer wavelength statistics and thus provide for the timely definition of performance requirements for specific future applications.

*Contract NAS-5-1545 with Communication and Systems, Inc. (C&SI); Falls Church, Va.; CY 1968-69; provided for study and definition of advanced space experiments operating at millimeter wavelengths and electro-optical frequencies. As part of this effort the author directed C&SI support-type analysis which, together with his own study, enabled him to propose and define the experiments described in this document.

CONTENTS

CONTENTS (Continued)

LIST OF ILLUSTRATIONS

LIST OF ILLUSTRATIONS (Continued)

LIST OF TABLES

PROPOSAL FOR ADVANCED LA. .ROPAGATION EXPERIMENTS BETWEEN STABILIZED SYNCHRONOUS SATELLITES AND GROUND STATIONS, AT VISIBLE AND NEAR-INFRARED WAVELENGTHS

by
Erwin Hirschmann
Goddard Space Flight Center

SECTION 1

OBJECTIVES

It is proposed to fly laser experiments on board three-axis-stabilized synchronous spacecrafts (Reference 1). These experiments will use wavelengths in the visible and near-infrared spectrum, and will consist of the following measurements:

a. A measurement of the propagation characteristics of an uplink at a near-infrared wavelength (i.e., 1.06 micron).

b. A measurement of the propagation characteristics of an uplink at a visible wavelength (i.e., 0.53 micron).

c. Round-trip characteristic measurements from ground stations, using an array of cubecorner retroreflectors on the spacecraft. The usable wavelengths for this experiment will include the entire visible spectrum and near-infrared spectrum.

Toward this end, spacecraft are required to carry two optical receivers at visible and near-infrared frequencies, respectively. In addition, an array of cubecorner retroreflectors will be flown to serve in round-trip propagation characteristics measurements and communication experiments, to be used as a passive target for laser radar, and/or to be used for improving the accuracy of tracking and spacecraft attitude control (References 2, 3, 4).

The main objectives of these advanced laser experiments are to initiate investigations of earth/space propagation and communication characteristics through the atmosphere at visible and near-infrared wavelengths, to study and demonstrate the technology to provide for possible increase in the usable spectrum available for earth/space communication needs, and to determine the trade-offs between the use of shorter and longer wavelengths for these communications.

A secondary objective of these laser experiments is to provide sufficient information on the possibility of using laser frequencies to improve the accuracy of navigation, tracking, and attitude control of spacecrafts.

If the state-of-the-art permits a spacecraft to facilitate a laser transmitter at 0.53 and/or 1.06μ wavelengths, an optional experiment, consisting of measurements of propagation characteristics of a downlink transmission, will be added. Once established, a communications downlink might be used to transmit data collected in a spacecraft from an uplink experiment, and help relieve the telemetry channel of some of its functions.

SECTION 2

BACKGROUND

The requirements for frequency allocations for point-to-point communications have increased exponentially in recent years. Prospects for the future are not optimistic unless the available spectrum can be extended.

Present earth/space communications use frequency bands usable for terrestrial communications. One way to increase the availability of frequencies for earth/space communications is to investigate the use of frequency bands not used for terrestrial links.

Some ATS experiments are being conducted to investigate the propagation characteristics of millimeter-wave frequencies through the atmosphere, for use in earth/satellite communication links.

The next step is the use of electro-optical wavelengths for communications between earth and space. Advantages of such wavelengths, as generated by lasers, include wide bandwidth capabilities, reduced spectrum occupancies, high-gain and small aperture antenna characteristics, light weight and reduced size of equipment components. The small aperture of the laser beam also limits the possibility of interference between users and might be highly desired in order to limit interception by undesired receivers and improve the security of the communication link. Laser experiments (Figure 1) are currently being implemented at the longer wavelength of 10.6 microns. Short

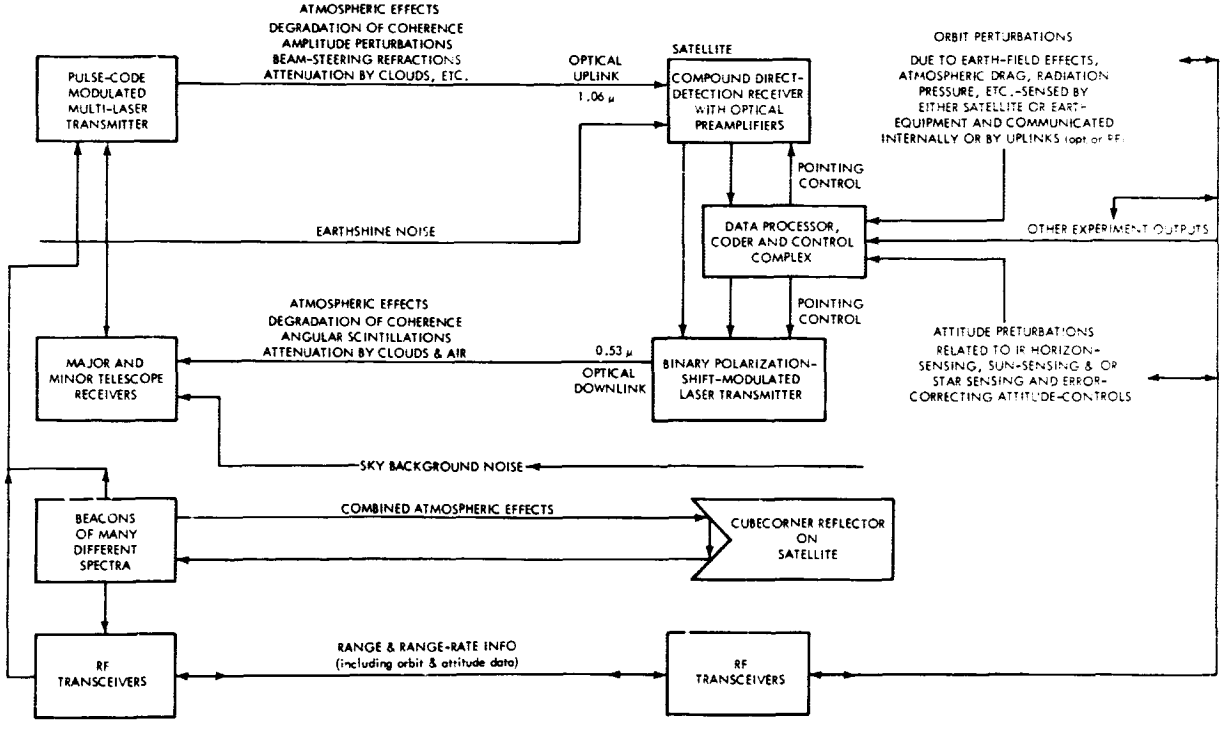

Figure 1—Block diagram of experiment.

wavelength experiments at the 1.06 micron and 0.53 micron region should also be conducted to provide complete statistical information.

The objective of the laser experiments is to provide sufficient data about the propagation characteristics of the earth's atmosphere in vertical or near-vertical links between earth and space.

Ground experiments have been conducted to determine atmospheric propagation data on horizontal paths at laser frequencies (Reference 5). Because of the structure of the atmosphere, vertical and horizontal characteristics are expected to differ greatly. For instance, propagation characteristics are very dependent on the structure of the refractive index of the medium. One of the most important factors affecting the refractive index is temperature. It has been shown (Reference 6) that the first 100 meters of the atmosphere is characterized by a marked diurnal variation of temperature gradients, with vertical gradients being orders of magnitude greater than horizontal gradients. Other meteorological and climatic factors play important roles in predicting optical beam degradation by the atmosphere. Such factors are turbulence parameter, presence of humidity in the form of haze, fog, cloud or rain along the path of the beam. The next section deals in more detail with the atmospheric effect at optical wavelengths and the choice of frequencies for earth/space communications links.

The optional downlink experiment will emphasize the difference in characteristics between uplink and downlink propagation. It is expected that the atmospheric effects, which are more important in the lower atmosphere, are different for the beam of a ground transmitter and for the beam of a downlink transmission near the receiver (References 7, 8).

Visible and near-infrared wavelengths (1.06 micron and 0.53 micron) need to be compared with infrared wavelengths (ex: 10.6 micron) and the trade-offs must be studied. Experiments (Reference 9) have been designed for 10.6 micron wavelengths; these will provide data for comparison with short wavelength type links operating between ground and spacecraft or spacecraft-to-spacecraft. Experiments using 1.06 micron and 0.53 micron wavelengths should be implemented to effect the needed comparison.

SECTION 3

SYSTEM DESCRIPTION

This section reviews the proposed laser experiments as being one complete overall short wavelength experiment, implemented as a single item and flown on board one spacecraft of modest capability. In practice, a series of experiments could be flown on board several less sophisticated spacecrafts. It describes the general characteristics of experiment implementations and operations. The next section describes the optical hardware in greater detail.

These laser experiments are designed to determine the propagation characteristics of the earth-spacecraft channel through the atmosphere, at visible and near-infrared frequencies. The propagation characteristics will be determined from analysis of the perturbations of probing signals transmitted through the channel at these frequencies. Test signals will be used on uplink and optional downlink carrier. The uplink receiver data is transmitted to the ground through the spacecraft wideband data and telemetry links, and stored on magnetic tapes for processing. The downlink receiver data and retroreflector data are likewise stored on magnetic tapes for later processing. Extensive meteorological data will be accumulated at each site including radar return, rain rate, wind velocity and direction, ambient temperature and pressure, relative humidity, and other measurements.

Several sites in the United States (Reference 10) will be utilized as laser ground stations, including a transportable station planned by GSFC for operation in any locality where it is deemed important to acquire data for specific weather profiles.

Participating ground stations situated in the area illuminated by the satellite transmitter antenna will be able to receive the optional downlink signal. All of the participating stations will be able, however, to transmit and receive simultaneously when operating with the retroreflector array if they are separated by a minimum distance.

3.1 Acquisition and Pointing

Factors of prime importance affecting signal acquisition and mechanical pointing of the receiving optics include the spacecraft attitude stabilization; perturbations on the satellite orbit due to sun, moon and earth oblateness; and the receiver platform stability. In addition, the atmosphere will cause a certain amount of time-varying distortion of the wave phase front.

3.2 Experiment Location and Constraints

On board a single technological type spacecraft an "all encompassing" experiment would be located in the Earthviewing Module, in a volume not exceeding 2 cubic feet. The available power of a suitable technological type spacecraft similar to the ATS series would limit the consumption to about 50 watts, with possible peaks of 100 W.

The spacecraft equipment, including the retroreflector array, will not weigh more than 40 or 50 pounds. This constraint might, however, limit the possibility of modulation and demodulation of the laser beams.

SECTION 4

OPTICAL TECHNOLOGY

4.1 Transmitters

4.1.1 Coherent radiation sources

The 1.06-micron (near-infrared) primary wavelength and the second-harmonic-generated (SHG) 0.53-micron (visible) wavelength have been arbitrarily specified as the radiations to be used for the laser experiments. Those wavelengths happen to be characteristic of the outputs from Nd:YAG laser crystals.

Assuming initially 12 watts output at 1.06 microns, or more than 6 watts output at 0.53 micron, operation in the diffraction-limited TEM_{00} (lowest-order) mode will have allowed the material's maximum gain (~2% per cm) to be approached. The Nd:YAG lasing medium, being solid-state, requires less volume* than gaseous types require, and it is supposedly less subject to deterioration over the average life of 1500 hours. Lifetimes of 10,000 hours are believed to be achievable in the near future, and higher output power levels should be obtainable with longer, redoubled resonant trains and with more efficient usage of the typical pump-lamp powers of around 3 kW that are already available (Figure 2).

Output efficiencies (References 11, 12) (now 0.4% and 0.2% for the 1.06 and 0.53 micron wavelengths, respectively) may be considerably improved by better spectral matching of new lamp types with chemically broadened pumping bands in the crystals. (Solar pumping is not depended upon because of its diurnal nature.) Recent advances in growing longer single crystals of any desired shape, together with more brilliant pumping light upon optically coupled rod assemblages, offer great promise.

CW oscillation is sometimes employed in order to realize bit rates as high as 10^6 per second. Mode-locking of the CW laser, particularly of the 0.53-micron SHG operation of a Nd:YAG crystal, could also produce a substantial enhancement in the average power output because of the square-law relation between fundamental and second-harmonic power levels.

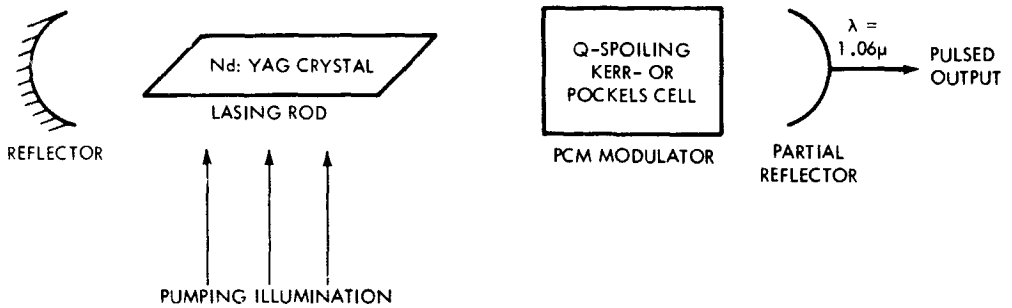

Figure 2—Schematic diagram of basic pulsed laser.

*Present cylinder measurements are 5 cm x 0.6 cm.

Some penalties are introduced, however, if CW oscillation and also binary polarization or phase-shift FM are employed in a satellite. The necessary temperature control of the laser—at 30°C for the 1.06-micron output, or at 80° ± 0.2°C for the SHG phased-matched Ba_2 Na Nb_5O_{15} crystal in the cavity for the 0.53-micron output—becomes a serious problem in a spacecraft because of power, weight and vibration features of the usual flowing-liquid heat-exchanger system. Ground-based operations obviously would not be so affected.

On the other hand, if higher-powered, pulsed operation is to be utilized instead, to satisfy the bandwidth and SNR relationships, then equally serious problems for satellite use may be associated with the sudden discharging and "ringing" of condenser banks. To get around the influence of any system vibrations up to at least 10 hertz, the pulse repetition rate of a Q-switched, high peak power laser must be in the order of 100 pulses per second; the angular divergence of the beam should not exceed 10^{-4} radian, and the pulse width should be from 10 to 20 nanoseconds (ns). These conditions do appear to be within reach during the allowed R&D time frame.

The technique of Q-spoiling, by itself, is effective in creating pulses only as short as $\sim 10^{-8}$ second in crystalline lasers, which limits earth-satellite range resolution to about 1.5 meters. If mode-locking were combined with Q-spoiling in such a laser, though, the structured main pulse of perhaps 5 to 12 elements (each no longer than 3×10^{-11} second) would theoretically give range resolutions down to a few centimeters or less. Such resolution, however, would exceed the accuracy which is allowed by the present uncertainty of knowledge concerning the speed of light.

That very uncertainty in the value of c is somehow tied to the consistent trend in determinations from the earliest generally accepted measurements in the optical region to the more recent ones in the microwave region—a trend believed to exceed the statistical errors and historical differences in parameters involved. Because of the distinct possibility that the speed of photons may soon be proved to be slightly frequency-dependent even in vacuum (by virtue of the ever present gravitational fields), just as it is definitely known to be in passing through the local fields of matter in more or less dispersed states, it becomes highly desirable to make *simultaneous* range measurements with optical, infrared, millimeter- and microwave radiations using picosecond pulse trains.

This particular test, barring atmospheric complications, could be done at any future time only through the use of a single, extremely broadband retroreflector on the satellite. In conjunction with this use of a common retroreflector, it would be necessary to determine very carefully the site displacements on the ground for the different, mutually phased, interferometer-type receivers of the respective return beams.

4.1.2 Modulations

The needs, kinds, and possibilities of modulation appropriate to the ground-based laser transmitter and to the satellite-borne optical transmitter are different. Some restriction upon the candidate methods, however, can be made by observing that the systems based on biorthogonal phase-shift-modulated emission and its heterodyne detection—preferred for far-infrared radiation around 10.6 microns wavelength—are less favored in the visible and near-infrared region, where binary polarization processes are advocated for direct-detection methods.

4.1.2.1 Satellite-borne modulation subsystem

To achieve high modulation rates and coding thereof at the 0.53-micron wavelength of the downlink, an electro-optic modulating crystal (such as the $Ba_2NaNb_5O_{15}$-SHG crystal already mentioned) is considered to be one of the most promising means. Such an acoustically damped, electro-optic crystal modulator would be most appropriate for satellite generation of the downlink 0.53-micron harmonic radiation, assuming combined Q-spoiling and mode-locking, since driver power and insertion loss are lowest for this reactive, optically non-absorbing component. The output becomes binary circularly polarized (RH - 0, or LH - 1) upon the inclusion of a quarter-wave plate in the optical train—a feature that avoids angular alignment problems between transmitter and receiver (Figure 3).

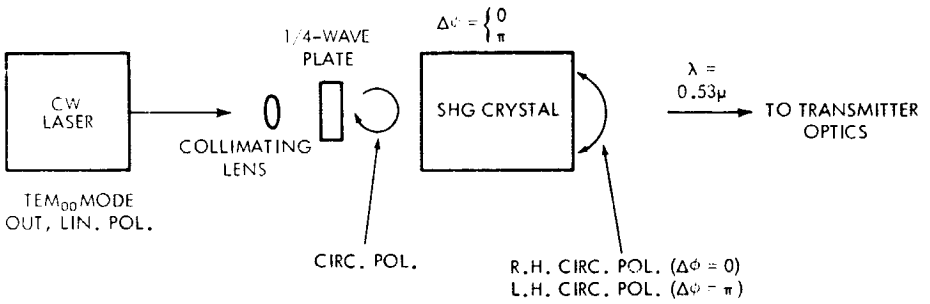

Figure 3—Schematic diagram of binary polarization-shift electro-optic modulator.

4.1.2.2 Ground-based modulation subsystem

Higher average Pulse Repetition Frequency (PRF) and wider variations of interpulse timings than are possible with a single source can be obtained for PPM or PIM modulation (References 13, 14, 15) by high-speed switching and sequencing of multiple laser sources. Such a system uses nitrobenzene Kerr- or Pockels cells and/or cavity-dumping calcite prisms. Because of the larger power and volume requirements of this multiple-source arrangement, it is naturally more suitable for the ground-based transmission of the primary 1.06 micron uplink. Polarization modulation may or may not be added to such a scheme, as the satellite-borne receiver would become quite complicated for the complete treatment (Figure 4).

4.1.3 Transmitter optics

4.1.3.1 Earth-beacon optics

Laser tracking and ranging of retroreflector-equipped satellites has already been practiced in a number of cases, so the issue is one of optimization for communication purposes rather than one of proving fundamental feasibility of beacon requirements.

It appears that the variable beamwidth of an earth-based beacon can be initially on the order of 0.1 milliradian to permit the acquisition of the satellite with full confidence of illuminating it,

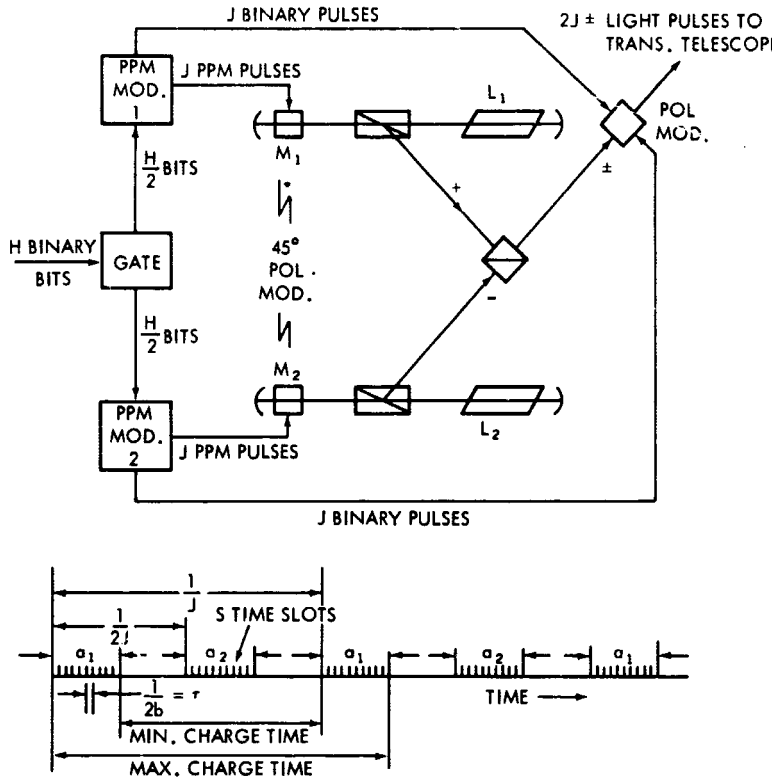

Figure 4—Two-laser system for a combined PPM and polarization-modulated CW pumped transmitter.

using standard tracking information and ephemeris data. This beamwidth would be satisfactory for exploratory communication only if a high pulse rate were employed with the presently available power level. Such a high signal level during the acquisition phase is advisable because the beacon's energy is spread out by the "floodlighting" requirement, partly to counteract random beam-steering refraction effects by the atmosphere near the transmitter. Fluctuations in the earthshine background at synchronous altitude, which averages about 5 watts/m^2, might otherwise introduce significant false-alarm rates or primary figure errors dependent upon the receiving aperture, gating, and pointing offset.

The desired pulse rate for carrying the information traffic at present power levels is still beyond the capability of individual lasers at the stated frequency. The multiple-source, "Gatling-gun" arrangement therefore merits serious consideration. It also means that the design of an earth-based transmitter must be radically different from conventional telescope types (such as previously proposed 24-inch aperture systems with diffraction-limited optics which must be de-focused to give a 10 arc-second beam divergence from a single laser) (Figure 5).

A suggested design would utilize a central deflector to feed all the radial inputs into a forward-channeling, somewhat ellipsoidal, mirror-walled tube with a center-stop in the form of a spindle-shaped mirror (Reference 16). For use with a circular array of near-infrared sources, such a

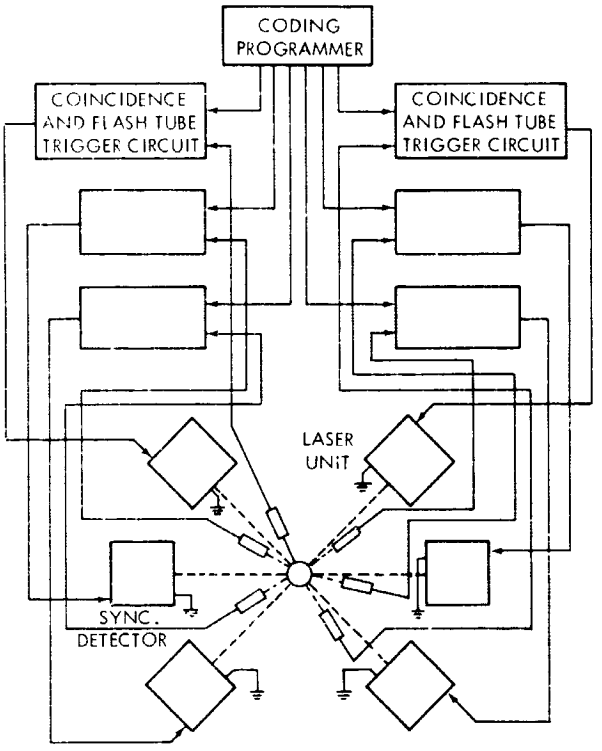

Figure 5—"Gatling-gun" arrangement for multiple laser source.

system employing total reflection at grazing angles has many advantages over a simple back-reflecting paraboloidal mirror, and especially over a refracting lens system. These advantages include, among others, easier preparation and maintenance of true surfaces; lightness, yet stability; no absorption or attenuation by back-scattering surfaces; and better control of aperture effects, variable beam focusing, and overall emission pattern. Pointing accuracies can easily be kept in the neighborhood of 5 arc-seconds (Figure 6).

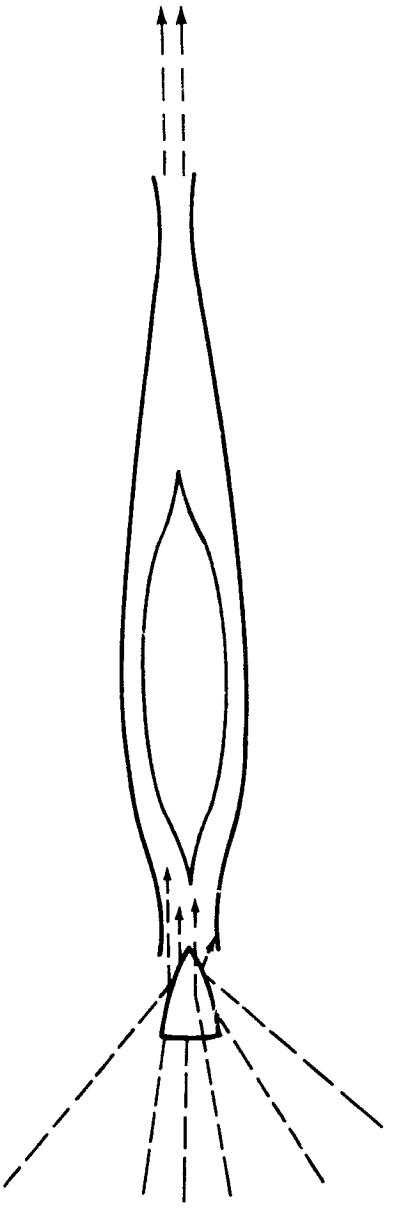

Figure 6—Reflective beam-projector for multiple laser source.

4.1.3.2 Satellite-beacon optics

Inasmuch as the transmitting optics in orbit need not and should not have the same characteristics as the satellite's collecting optics used to receive the earth beacon, two separate systems are recommended. As much of the burden as possible should be placed on the ground facilities, so it is fortunate that only a 7-inch-aperture Questar telescope is calculated to be necessary for delivering the 0.53 micron output of the satellite-borne SHG—Nd:YAG laser (Figure 7).

Such a telescope normally has high-quality diffraction-limited optical components, and the substitution of new fused-silica materials with ultra-low expansion coefficients would be the only change suggested for space qualifications. The pointing of a sharp, fine beam to an accuracy within 1/10 of the beamwidth is the main requirement, so it is well that there are no atmospheric disturbances near the transmitter in the downlink situation. It is assumed that the uplink beacon reference (or alternatively, RF communications) will provide guidance in closing the optical communication loop through directional cues to the attitude-control mechanisms for both the telescope and its platform (Figure 1).

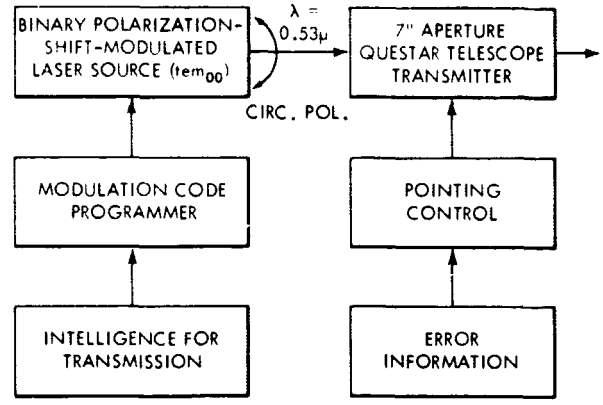

Figure 7—Block diagram of satellite-borne laser transmitter.

4.2 Receivers

4.2.1 Uplink reception

The coherently correlatable regions of near-infrared (and visible) wavefronts exhibit greatly reduced dimensions after passing through the turbulent atmosphere to a satellite. Direct-detection, incoherent receivers capable of efficient beam collections are consequently indicated here, instead of smaller heterodyne or homodyne systems (which, incidentally, require precise co-alignment and frequency characteristics of the beam from a local oscillator) (References 15, 17 to 25).

The proposed multiple-source, high intensity, rapid-fire coding of the 1.06-micron uplink beacon has the advantage that it can be designed so that received demodulation and interpretation of the essentially incoherent beam need not be constrained to decoding techniques in which binary decisions are made just on the basis of the presence or absence of individual pulses (with the attendant 2 dB penalty relative to coherent detection methods). Rather, more complex step-functions and other pulse-code-modulated (PCM) signal properties and redundancies may be utilized at will, since power, average PRF, and variable interpulse-timing demands are readily met by the multiple-source arrangement on the ground. The PCM method of communicating signals unquestionably offers the greatest potential for reducing the ratio E/N_0 to 0 dB in this uplink system.

It is generally accepted that incoherent, direct-detection optical receivers may employ large, non-diffraction-limited collecting apertures, since their cross-section is not limited by the aerial dimensions of finite coherence dictated by atmospheric turbulence. In fact, if whatever gain that is sacrificed by employing an array of smaller apertures instead of a single large collector can be more than made up by using separate pre-detection amplifiers, then the almost insurmountable problem of assuring extremely rigorous optical-mirror tolerances over one large surface on a

spacecraft can be circumvented. Moreover, the use of a collection of individual directional receivers optimizes the capability of detecting any pointing and offset errors during reception of the earth beacon (Figure 8).

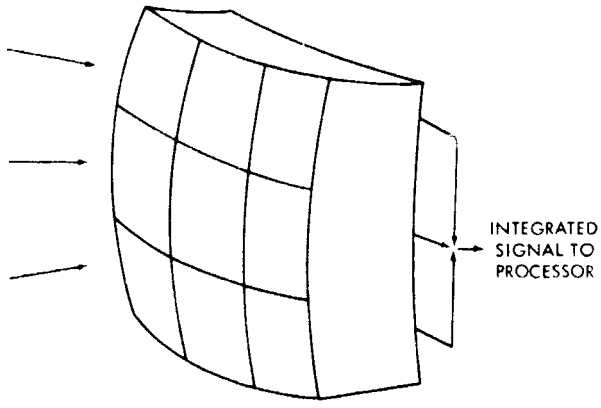

Figure 8—Possible eggcrate array of radiation collectors for satellite-borne direct-detection receiver.

An optical amplifier with low spontaneous emission would make the relative effects of thermal and shot noise negligible upon final photodetection of the signal; the overall performance of a given receiver would thus be independent both of transmission losses in its optical elements and of the quantum efficiency of the detector.

The prevailing opinion, however, has been that there are no adequate pre-detection amplifiers for use with near-infrared or optical receivers. That is no longer true with the advent of night-flight-tested, extremely sensitive, signal-intensifying electroluminesant panels capable of great gain at very low fluxes of incident photons (References 26 to 30). These new, thin panels—which combine the highly efficient photon-counter features of sensitive, solid-state photoemissive films with intense Townsend-avalanche amplification by gaseous microchannels—are able to enhance spatially discrete images preferentially over noisy backgrounds without requiring cryogenic cooling. But there is really no need for engineering the receiver surfaces to precisely focus sharp images of the earth-based beacon source, so long as the compound collecting system simply registers a common signal pulse.

It is thus sufficient to have an array of moderately small, lightweight, solar-furnace-type collectors, each giving a relatively unsharp focal spot. The near-infrared radiation included in one-meter-diameter segments of the incident wavefront can be reflectively concentrated onto intensifying panels of as much as 3 to 9 cm cross-dimension. The practical magnitude of the sensitive area of this type of pre-detection amplifier is not a design-restricting factor, as it would be for refractive coupling into the narrow receiving end of an inherently inefficient laser amplifier (Figure 9).

It is essential, of course, to narrow the pass-band of radiation to be accepted by the preamplifying panel, in order to reduce the background noise outside the signal band. This can be done by inserting a pre-detection filter in front; but, in doing so, latitude must be allowed for Doppler frequency shifts and the filter must be characterized by low signal absorption and low self-emission noise. These requirements are well satisfied by a thin-film interference filter consisting of a set of many alternate quarter-wave layers of high and low refractive index dielectric films that are separated from a similar set by a half-wave dielectric spacer. This type of filter gives extremely high transmission at the peak of a properly finite pass-band and it also allows some tunability by slight changes in the angle of incidence. The technology of producing thin-film interference filters

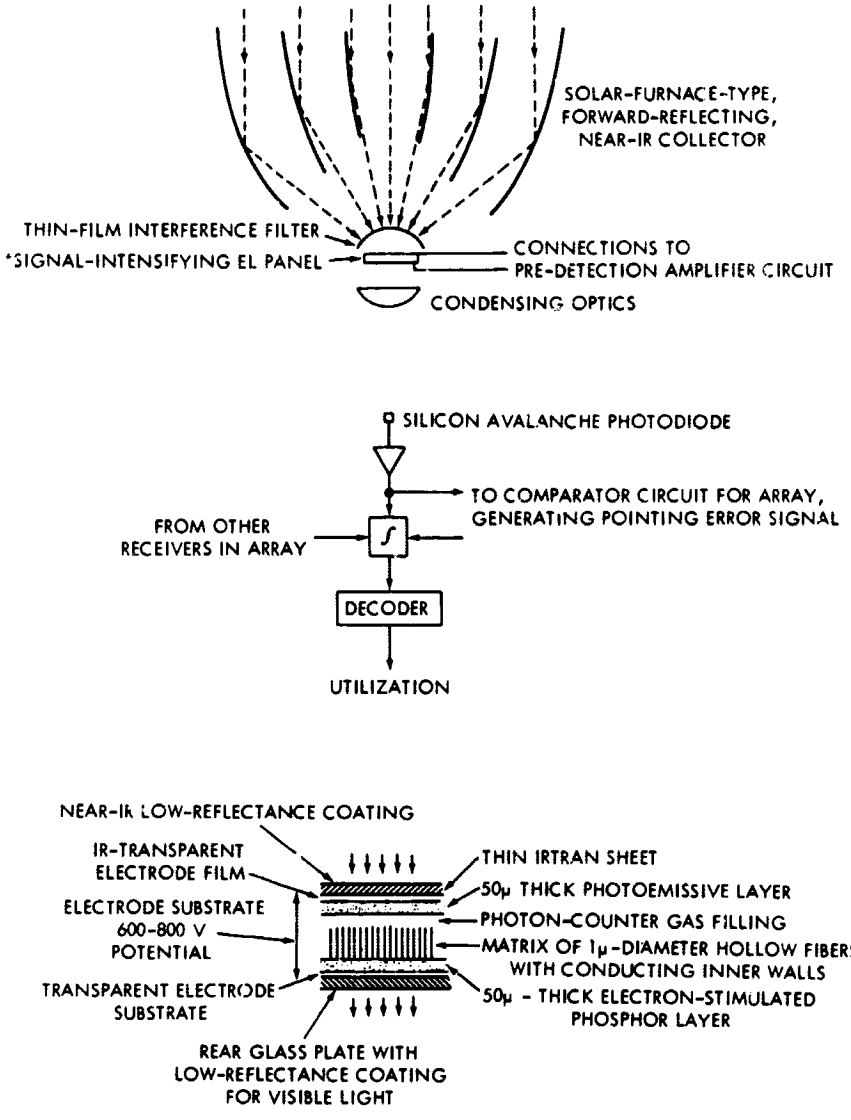

*ENLARGEMENT OF ELECTROLUMINESCENT PANEL (patent applied for by Systems Dynamics, Inc.)

Figure 9—Direct-detection receiver with optical preamplifier.

in the near-infrared for large apertures is, fortunately, the most advanced of all optical filter technologies.

The next components to follow the sequence of reflective radiation collector, filter sheet, and preamplifier panel in the satellite-borne receiver should be a strongly condensing lens system and a solid-state photodetector element. The optical elements do not have to be IR-transparent, since conversion into visible frequencies will have been performed by the electroluminescent output layer of the panel. The photodetector element may be as small as 0.04 mm in diameter without

compromising this optical system in any way, and it has the favorable properties of ruggedness, wideband input, low weight, low power needs, and relatively noise-free, reliable output over a long lifetime. The quantum efficiency of a silicon avalanche photodiode in the visible region is notably high, and its internal amplification factor may be as much as 100-fold.

The output of the photodetector element in each receiver within the compound system is individually amplified before being centrally integrated, decoded, and channeled. The minor amplification step enables tap-off sampling of the respective receiver signals before they are combined, for the purpose of determining any radiation-pattern imbalance due to pointing error of the whole receiver complex and/or satellite platform.

4.2.2 Downlink reception

The incoherent communication of visible 0.53-micron radiation from the synchronous satellite to a ground station will require an ordinary 24-inch telescope receiver with both Coudé focus and conventional focus. Around the main telescope there should be at least four 6- to 12-inch slave telescopes located at the -3 dB radial points of the far-field intensity pattern, so as to provide the information for correcting any pointing and tracking errors (Figure 10).

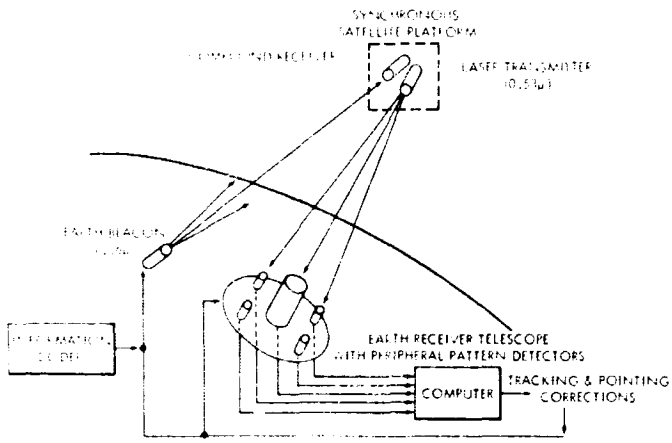

Figure 10—Active transceiver network for laser communications.

Due to the geometric aberration introduced by the relative velocities of the system end-points, plus the possibility of local scattering interference, it is advisable to separate the ground receiver from the ground transmitter. The angular velocity aberration of a synchronous satellite is approximately 3.60 arc-seconds (17.4 microradians), which is equivalent to a separation of 2045 feet on the earth's surface. In fact, a considerable diversity of receiving sites would be logical for the sake of uninterrupted reception in case of bad weather over any one or more of the sites. This assumes a re-pointing capability for the satellite-borne transmitter upon change-over to a new uplink beacon and cessation of the old one.

The binary polarization-shift modulation of the transmission from the satellite at the 0.53-micron wavelength calls for a direct-detection receiver with a narrow pass-band filter and a polarization separator following the telescope optics. The polarization separator divides the incoming radiation into the two orthogonal polarizations employed by the transmitter (circular, in preference to linear), each being detected and processed by its separate chain of photomultiplier, amplifier, integrating comparator, decoder, etc. Current at the output is time-averaged for a bit period, and the selection decision is based on which channel has the larger average current (Figure 11).

Photomultipliers (Table 1) with S-20 photocathodes are probably satisfactory for this system. In such a case, the current at the output of the detector is sufficiently large that detector dark current and Johnson noise may be neglected. The dominant noise term is then signal shot-noise or quantum noise, which is present only when the signal is present. The quantum efficiency of the S-20 photoemissive surface at 0.53 microns is 0.20.

In addition to the detector loss, there will be losses in the optical filter and polarizer. The main purpose of a predetection filter is to increase the signal-to-noise ratio of the radiation on the detector. In this set-up, a Fabry-Perot filter can be effectively employed, as it produces a narrower passband with a higher band transmission than either the thin-film interference filter or a birefringent filter, and it is also tunable to allow for Doppler shifts. Although the basic construction of the Fabry-Perot filter is the same as that of the thin-film type (except that the spacer thickness is an integral number of half-wavelengths), an additional blocking filter of the thin-film type must be used to mask out unwanted passbands. There is no requirement here for coverage of a large area, since the rays from the telescope converge to a reasonably sharp focus.

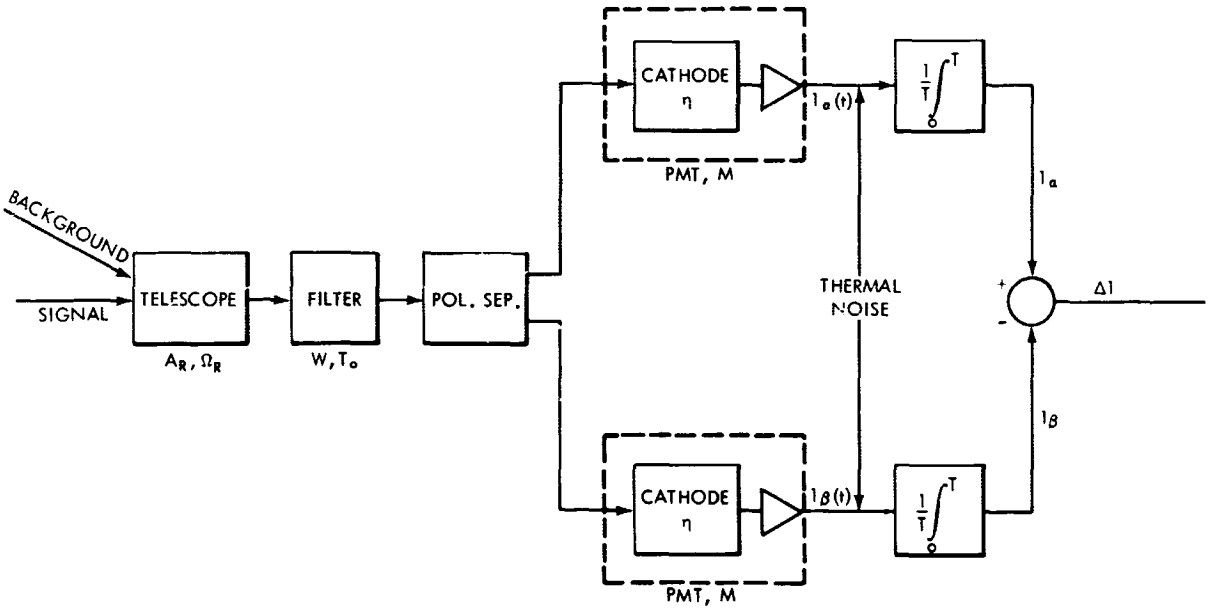

Figure 11—Schematic representation of direct-detection receiver for binary polarization-shift-modulated downlink (0.53μ).

Table 1

Photocathode Table (after ITT data chart).

Device S-Number	Photocathode Components	Window Material	Photocathode Support	Luminous Sensitivity (A/lm)	Dark Current at 25°C (A/cm^2)
S-1	Ag-O-Cs	Visible light transmitting glass	Entrance window or opaque material	25	10^{-11} to 10^{-13}
S-3	Ag-O-Rb	Visible light transmitting glass	Opaque material	6.5	10^{-12}
S-4	Cs-Sb	Visible light transmitting glass	Opaque material	40	10^{-14}
S-5	Cs-Sb	Ultraviolet light transmitting glass	Opaque material	40	10^{-14}
S-8	Cs-Bi	Visible light transmitting glass	Opaque material	3	10^{-14} to 10^{-15}
S-9	Cs-Sb	Visible light transmitting glass	Entrance window	30	10^{-14}
S-10	Ag-Bi-O-Cs	Visible light transmitting glass	Entrance window	40	10^{-13} to 10^{-14}
S-11	Cs-Sb	Visible light transmitting glass	Entrance window	60	10^{-14} to 10^{-15}
S-13	Cs-Sb	Fused silica	Entrance window	60	10^{-14} to 10^{-15}
S-17	Cs-Sb	Visible light transmitting glass	Opaque material	125	10^{-14} to 10^{-15}
S-19	Cs-Sb	Fused silica	Opaque material	40	10^{-14}
S-20	Sb-K-Na-Cs	Visible light transmitting glass	Entrance window	150	10^{-15} to 10^{-16}
S-21	Cs-Sb	Ultraviolet light transmitting glass	Entrance window	30	10^{-14}

SECTION 5

ATMOSPHERIC EFFECTS: OPTICAL ATTENUATION BY CLOUDS, HAZES AND RAIN

Very few portions of the earth remain unobscured from hazes and clouds for extended periods, so optical communications over certain paths through the earth's atmosphere can become marginal or even impractical. Furthermore, even some "clear air" atmospheric conditions are not particularly conducive to reliable and efficient optical communications, owing to "poor seeing" conditions. These factors are well known in general; however, the optical properties of major clouds and the relationship between "poor seeing" and meteorological conditions have not been amply treated in the literature.

The percentage frequencies of cloud cover (6/10 to 10/10) over the northern hemisphere are shown in Appendix A, Figures A1 through A9, for various cloud types, incremental altitudes, and seasons (Reference 31). The probability of a clear line of sight through the clouds depends upon the relative vertical and horizontal dimensions of the cloud structure. The probability is high that a cloud will intercept and partially obstruct an optical beam in transit through the atmosphere, depending on the communication terminal locations. The main question then is: "What are the attenuating properties of these obstructions?"

The optical properties of hazes and clouds can be computed using the exact Mie theory of electromagnetic wave scattering, providing the size, number, distribution, and index of refraction of the scatterers are known. The Mie theory is discussed lucidly and amply by van de Hulst (Reference 32). Typical size distributions of hazes and cumulus clouds are described by Deirmendjian (Reference 33) and their attenuating effects on visible and infrared radiation are calculated. Figure 12 shows the particle size distributions of both continental and maritime hazes, and of a cumulus cloud with a total concentration of 100 cm^{-3} (N is the total number of particles per unit volume.) Table 2 summarizes the spectral attenuation properties of these distributions. It is noted that, for scattering by hazes or small particles, infrared radiation surpasses visible light for transmission through the haze. On the other hand, clouds are comprised of larger droplets, and it is noted that their related optical

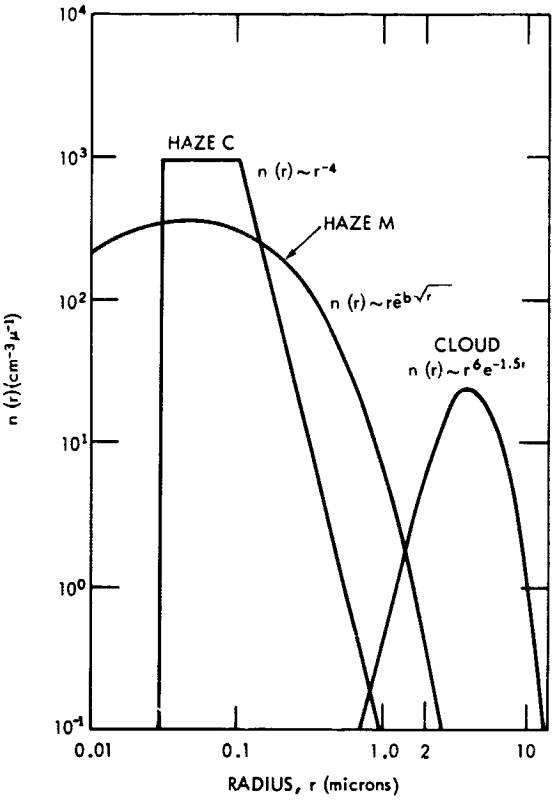

Figure 12—Three size-distribution functions used in the integration of the Mie functions.

extinction properties are relatively insensitive to wavelength. Figure 13 shows signal attenuation for different frequencies, in light fog and under various rain conditions.

Table 2

Attenuation of Optical Radiation by Hazes and Cumulus Cloud (Reference 33).

Wavelength (μ)	Continental Haze b_{ext} (m^{-1})	Maritime Haze b_{ext} (m^{-1})	Cumulus Cloud b_{ext} (m^{-1})
0.45	1.21×10^{-4}	1.06×10^{-4}	1.63×10^{-2}
0.70	7.59×10^{-5}	1.06×10^{-4}	1.67×10^{-2}
1.61	3.12×10^{-5}	6.91×10^{-5}	1.76×10^{-2}
2.25	1.94×10^{-5}	4.24×10^{-5}	1.82×10^{-2}
3.07	2.89×10^{-5}	6.02×10^{-5}	1.86×10^{-2}
3.90	1.28×10^{-5}	2.36×10^{-5}	2.06×10^{-2}
5.30	7.50×10^{-6}	1.12×10^{-5}	2.40×10^{-2}
6.05	1.29×10^{-5}	1.89×10^{-5}	1.99×10^{-2}
8.15	5.00×10^{-6}	6.20×10^{-6}	1.88×10^{-2}
10.0	3.20×10^{-6}	4.5×10^{-6}	1.12×10^{-2}
11.5	6.40×10^{-6}	9.70×10^{-6}	1.01×10^{-2}
16.6	8.20×10^{-6}	1.34×10^{-5}	1.70×10^{-2}

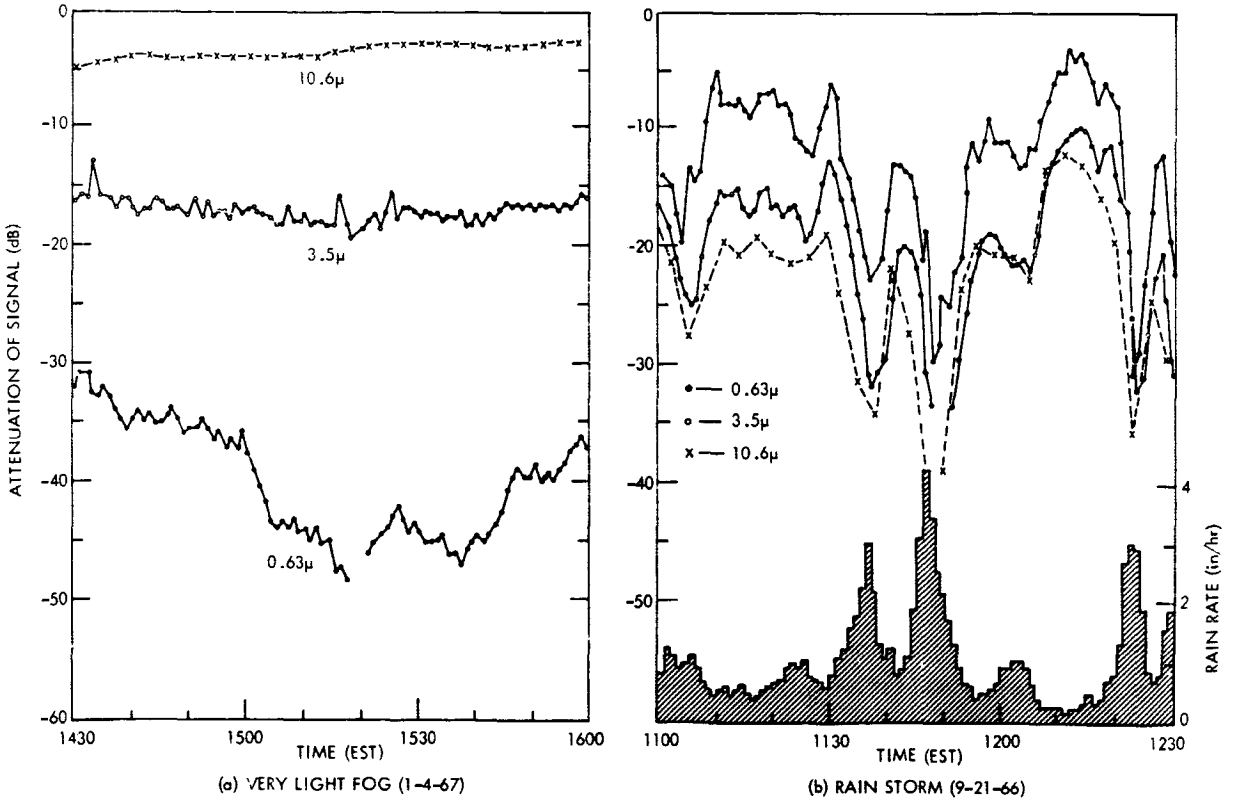

Figure 13—Measurement of 2.6-kilometer transmission loss relative to signal level (0 dB) in clear weather.

The cloud particle-size distribution of Figure 12 is not an all-encompassing cloud model; hence, the values of optical attenuation by clouds in Table 1 are not completely descriptive of the optical properties of the atmosphere. Cato, Carrier, and von Essen (Reference 31) conducted an extensive survey of the literature in order to establish representative cloud models for the eight major cloud types (comprised of water droplets); the conclusion of the study is that the cloud droplet spectra depicted in Figure 14 represent typical cloud models. The optical properties of these cloud models were computed, and optical scattering coefficients associated with the cloud models are summarized in Table 3. It is significant to note that optical extinction, due to the scattering processes, shows little dependence upon wavelength, in agreement with Deirmendjian's calculations; however, optical extinction can be appreciably higher than that predicted by Deirmendjian for his cumulus cloud model.

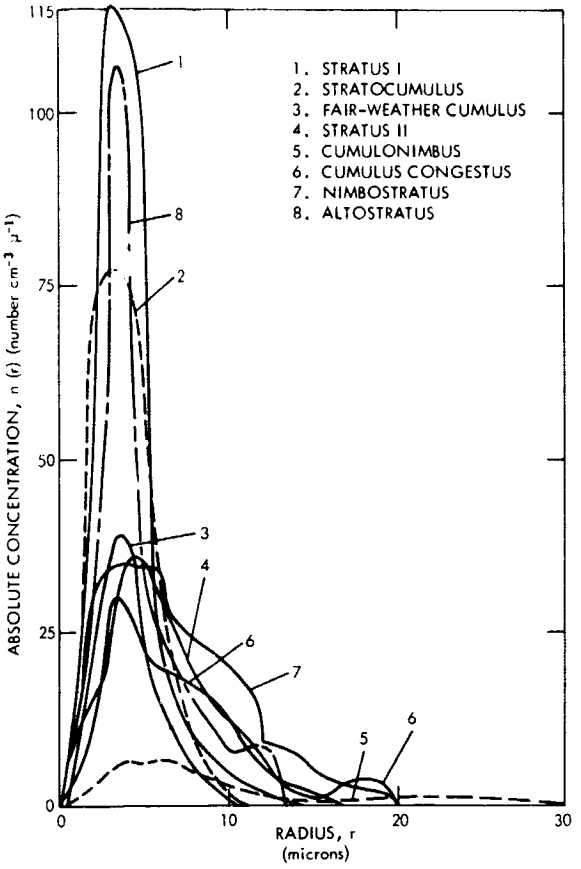

Figure 14—Model cloud drop spectra.

Another significance of the predicted values of optical scattering coefficients for clouds other than that of optical extinction is that multiple scattering effects can become appreciable, thus smearing an optical signal in time and intensity, with commensurate degradation of an optical system's communication efficiency. The problem is treated in part by Dell-Imagine (Reference 34).

Measurements performed in 1966 and 1967 on a 2.6 km path through fog and through rain storms indicate opposite influences of frequency variations. Figure 13a shows how high infrared wavelengths are transmitted through fog with less attenuation than near-infrared and visible wavelengths, though Figure 13b shows that infrared wavelengths are more attenuated by rain than are shorter wavelengths (Reference 15).

To conclude, this section has shown that optical attenuation by clouds is relatively insensitive to the wavelength (Table 2), that haze and fog attenuation is less for long wavelengths (Table 2 and Figure 13a), and that attenuation by rain storms, on the contrary, is less for short wavelengths (Figure 13b).

Table 3

Optical Scattering Coefficients, $b(m^{-1})$, of the Major Cloud Types.

Cloud Type	Wavelength				
	0.488μ	0.694μ	1.06μ	4.0μ	10.6μ
Nimbostratus	1.28×10^{-1}	1.30×10^{-1}	1.32×10^{-1}	1.47×10^{-1}	1.36×10^{-1}
Altostratus	1.08×10^{-1}	1.09×10^{-1}	1.12×10^{-1}	1.30×10^{-1}	8.39×10^{-2}
Stratus II	1.00×10^{-1}	1.01×10^{-1}	1.03×10^{-1}	1.14×10^{-1}	1.04×10^{-1}
Cumulus Congestus	6.92×10^{-2}	6.98×10^{-2}	7.13×10^{-2}	8.10×10^{-2}	6.76×10^{-2}
Stratus I	6.69×10^{-2}	6.79×10^{-2}	6.97×10^{-2}	9.01×10^{-2}	4.28×10^{-2}
Cumulonimbus	4.35×10^{-2}	4.38×10^{-2}	4.44×10^{-2}	4.82×10^{-2}	5.09×10^{-2}
Stratocumulus	4.53×10^{-2}	4.60×10^{-2}	4.71×10^{-2}	5.96×10^{-2}	2.48×10^{-2}
Fair-Wx Cumulus	2.10×10^{-2}	2.13×10^{-2}	2.19×10^{-2}	2.76×10^{-2}	1.17×10^{-2}

SECTION 6

DATA ACQUISITION AND PROCESSING

This section deals with the acquisition and processing programs of data for the laser experiment.

This experiment comprises two types of data analyses:

1. A statistical comparison of signal characteristics (amplitude and phase) with meteorological data such as temperature, relative humidity, refractive index, rainfall rate, radiometer temperature, weather radar return, and presence of fog or clouds.

2. A correlation analysis of the signal amplitude data, in time and frequency.

The first type would be referred to as the propagation data analysis while the second type would be called the signal correlation analysis.

All uplink data collected in the spacecraft, as well as housekeeping data, would be received under responsibility of a Command Station (such as ATSCOM).

An Operations Center (such as ATSOC) would be responsible for all activity coordination related to the satellite.

A transportable terminal (similar to the ATS-V Millimeter Wave Experiment prime station) would act as prime station, with the capability of receiving the optional downlink signal and transmitting the uplink signals at 0.53 and 1.06 micron.

A secondary station would be provided, with the capability of acting as alternate for the prime station, and thus capable of receiving and transmitting at the same frequencies. Other participants in the laser experiment would limit their capacity to receiving the downlink transmission only. The uplink and downlink transmissions are independent of each other. On the uplink, only one of the two transmitting stations can operate at a time, while on the downlink all receiving stations may participate simultaneously during transmission.

The retroreflector experiment would be treated independently. Participating stations would be allowed the use of the retroreflector array according to prescheduled programs submitted to the Operations Center for coordination and approval. The data processing program for the laser experiment will be designed to include a degree of flexibility to allow investigation of unusual occurances, yet sufficiently rigid to allow prearranged scheduling of the data reduction process, thus minimizing the conditions which usually result in long backlogs.

6.1 Meteorological Data Acquisition

Acquisition of extensive meteorological and supporting data would be planned for the transportable (or prime) station. The other participating stations would contain most of the

elements of the prime station, but in general, may not have the complete capability of the prime station.

The prime station would record the following meteorological measurements: weather radar integrated output, refractometer output, rain gauge rate, wind velocity and direction, ambient temperature, pressure and relative humidity, cloud coverage photographs, and photographs of the weather radar scope display.

6.2 Propagation Analysis

The recorded propagation data and meteorological data would be transferred to tapes, which would then be sent to a computer processing center where the principal data processing would be accomplished. These tapes would be utilized to generate charts based on daily, weekly, monthly, seasonal and yearly statistics. As each computation would be completed, a new set of records would be generated, which would average the previous data records into a compressed record. For example, after the daily charts are produced, five daily records would be averaged, (every five readings) to produce a weekly record of the same length. The same computer program could then be utilized to produce the weekly charts. A similar averaging procedure would be followed for monthly, seasonal and yearly chart generation.

A correlation analysis would be performed with analog data primarily for those periods when significant changes are noted in the signal parameters.

6.3 Signal Correlation Analysis

The correlation analysis would be performed on a multiplexed signal processor which would determine time autocorrelation and crosscorrelation of the signal outputs of the uplink and downlink receivers.

REFERENCES

1. Weinreb, M. B., "Preferred Approach for ATS F&G," GSFC Document, November 20, 1967.
2. Minott, P. O., "Proposal for ATS D or E Synchronous Orbiting Retrodirective Optical Communication Experiment," GSFC Document X-524-66-177, April 1966.
3. Dyson, J., "Optics in a Host'e Environment," *App. Optics* 7(4):569-580, April 1968.
4. Burckhardt, C. B., Collier, R. J., and Doherty, E. T., "Formation and Inversion of Pseudoscopic Images," *App. Optics* 7(4):627-630, April 1968.
5. "Program Specification Plan for the Determination of Atmospheric Effects on Laser Space Communications," Vol. II, SID 65-1467, North American Aviation Inc., Space and Information Systems Division, 9 November 1965.

6. "Study of Atmospheric Degradation of Laser Beams," EOS Report 7097-Final, Prepared for NASA-ERC under Contract NAS 12-130, December 1967. (NASA CR No. Cl-86030, Accession No. N68-16369).

7. Munick, R. J., "Turbulence-Produced Irradiance Fluctuations in Ground-to-Satellite Light Beams," SID 64-2222, North American Aviation Inc., Space and Information Systems Division, 28 December 1964.

8. Chang, N. C., and Brock, E. G., "Design Considerations of Multiple Laser Communication Links Between Synchronous Satellite and Several Earth Stations," Air Force Report No. SAMSO-TR-68-7, prepared by Aerospace Corporation, September 1967.

9. Plotkin, H. H., "Laser Tracking and Communication with Satellites," GSFC Document X-524-69-193, October 1968.

10. "NASA Reports on Survey to Find Site for Optical Communication Experimental Facility," *Laser Focus* 4(12):18, August 1968.

11. Heyck, H. D., "Sensor Problems in Space and Interplanetary Navigation," presented at the 12th East Coast Conference on Aerospace and Navigational Electronics, Baltimore, Maryland, 27-29 October 1965.

12. "Nd YAG Competes with Argon in Commercial Market," *Laser Focus* 5(9):16, May 1969.

13. Ross, M., "Visible and near-IR Laser Modulation," *Electro-Technology* p. 21-28, February 1969.

    Ross, M., "Jupiter Calling," *Laser Focus* 5(19):32-38, October 1969.

14. "Wideband Laser Communications," by Lockheed Corporation, Palo Alto, California, 1969.

15. BTL Space Communications Study (NASA Report, Chapters 1, 4, 5 and 6), Bell Tel. Labs. Contract NAS5-10293, May 1, 1968.

16. De, M., Lit, J. W., and Tremblay, R., "Multi-aperature Focusing Technique," *App. Optics* 7(3): 483-488, March 1968.

17. Lahti, J. N., "Detection of Narrowband Gaussian Optical Fields and the Incoherent Optical Heterodyne," Bell Tel. Labs. Tech. Memo 67-4133-11, Case 28503, March 1, 1967.

18. Lahti, J. N., "On the Directional Sensitivity of Optical Detectors," Bell Tel. Labs. Tech. Memo 67-4133-17, Case 28503, June 12, 1967 (with one appendix).

19. Bowen, J. I., "Optical Deep Space Communication: Polarization Modulation with Direct Detection," Bell Tel. Labs. Tech. Memo 67-4133-10, Case 28503, March 21, 1967 (with three appendices).

20. Jacobs, I., "Incoherent Detection of Optical Communication Signals," Bell Tel. Labs. Memo for File, Case 28503, Feb. 27, 1967 (with on appendix plus errata memo dated June 21, 1967).

21. Jacobs, I., "Heterodyne Detection of Optical Signals with a Phased Array," Bell Tel. Labs. Memo for File, Case 28503, May 23, 1967.

22. DeLange, O. E., "The Performance of Receivers Employing Light Amplifiers," Bell Tel. Labs. Tech. Memo 67-1246-8, Case 28503, March 21, 1967 (with one appendix).

23. Lasser, M. E., "Detection of Coherent Optical Radiation," *IEEE Spectrum* 3(4):73-78, April 1966.

24. Cooper, B., "Optical Communications in the Earth's Atmosphere," *IEEE Spectrum* 3(7):83-88, July 1966.

25. Brookner, E., Kolker, M., and Wilmotte, R. M., "Deep-Space Optical Communications," *IEEE Spectrum* 4(1):75-82, January 1967.

26. Yu, F. T. S., "Statistical Brightness Gain of a Channeltron Image Intensifier," *App. Optics* 7(8):1601-1607, August 1968.

27. Theodoron, D. G., "Research and Development of a Channeled-Electron Image Intensifier," *J. App. Physics* 36(5), May 1965.

28. "Electro-Optics," *Electronics Rev.* 41(19):54-55, September 16, 1968.

29. "Industrial Electronics," *Electronics Rev.* 41(12):62-64, June 10, 1968.

30. "The Greatest untold Story of Vietnam War," *Electro-Technology* 82(1):30-31, July 1968.

31. Cato, G., Carrier, L., von Essen, K., "Laser Systems Study, Part III: Effects of Clouds," Report 4440-Final III, (AD 479 487). Electro-Optical Systems, Inc., Pasadena, California, December 1965.

32. van de Huest, H., "Light Scattering by Small Particles," New York: John Wiley and Sons, 1964.

33. Deirmendjian, D., "Scattering and Polarization Properties of Water Clouds and Hazes in the Visible and Infrared," *App. Optics* 3(2):187, February 1964.

34. Dell-Imagine, R., "A Study of Multiple Scattering of Optical Radiation with Applications to Laser Communication," in *Advances in Communication Systems* (Vol. 2), Balakrishnan, A. V., Ed., New York: Academic Press, 1966.

APPENDIX A

CLOUD COVER DATA

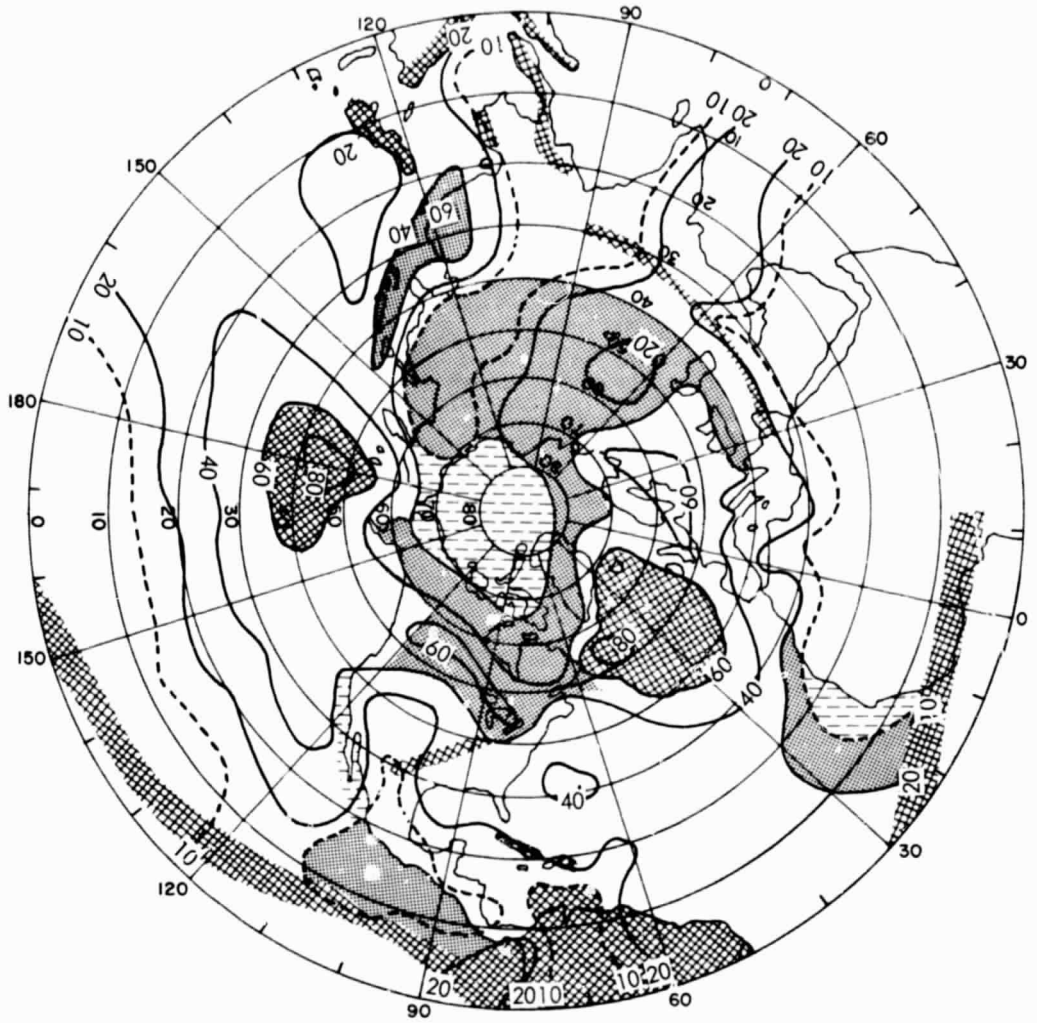

Figure A1—Percentage frequency of 6/10 to 10/10 cloud cover at altitudes from sea level to 5,000 feet (Winter).

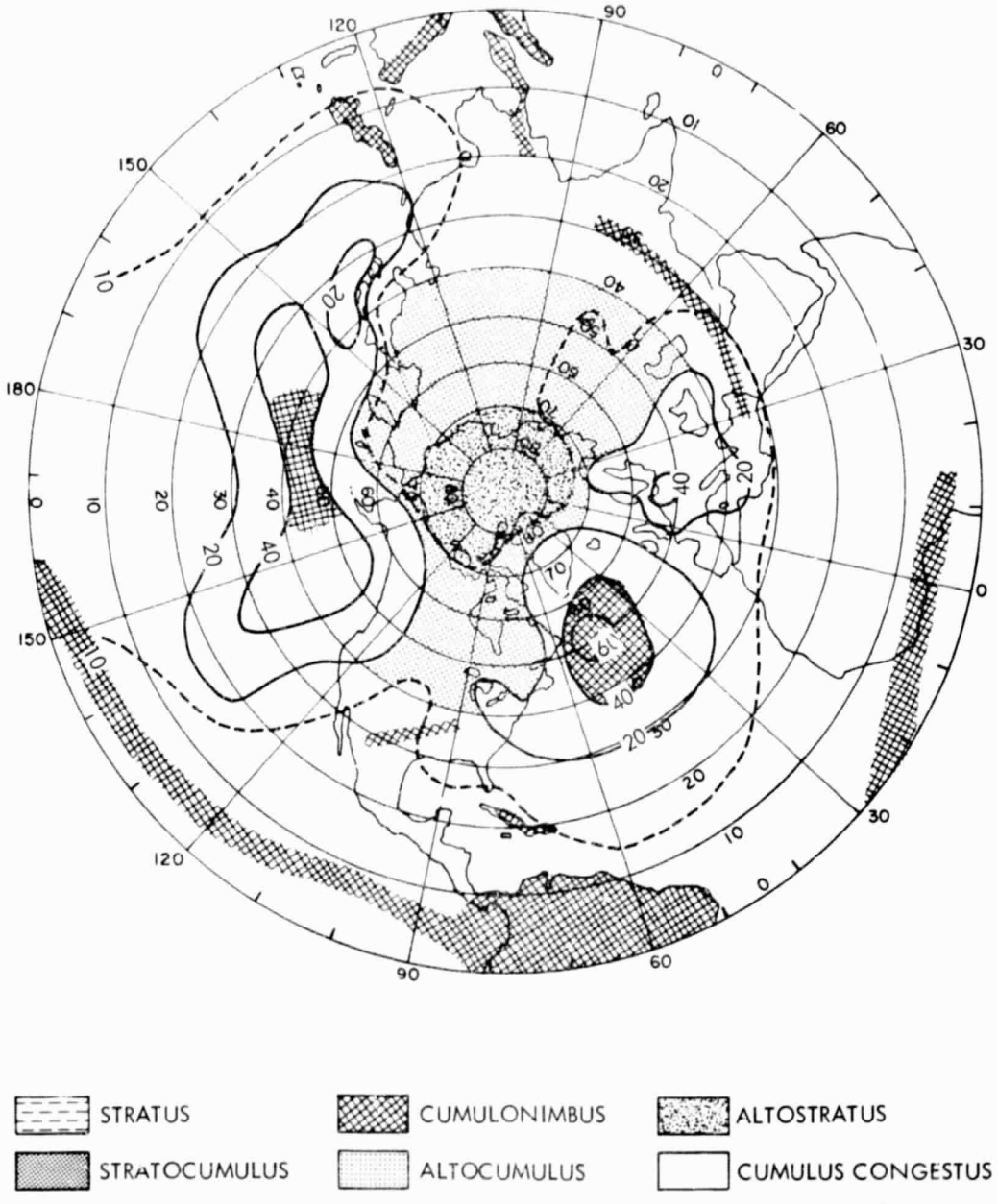

Figure A2--Percentage frequency of 6/10 to 10/10 cloud cover at altitudes from 5,000 to 10,000 feet (Winter)

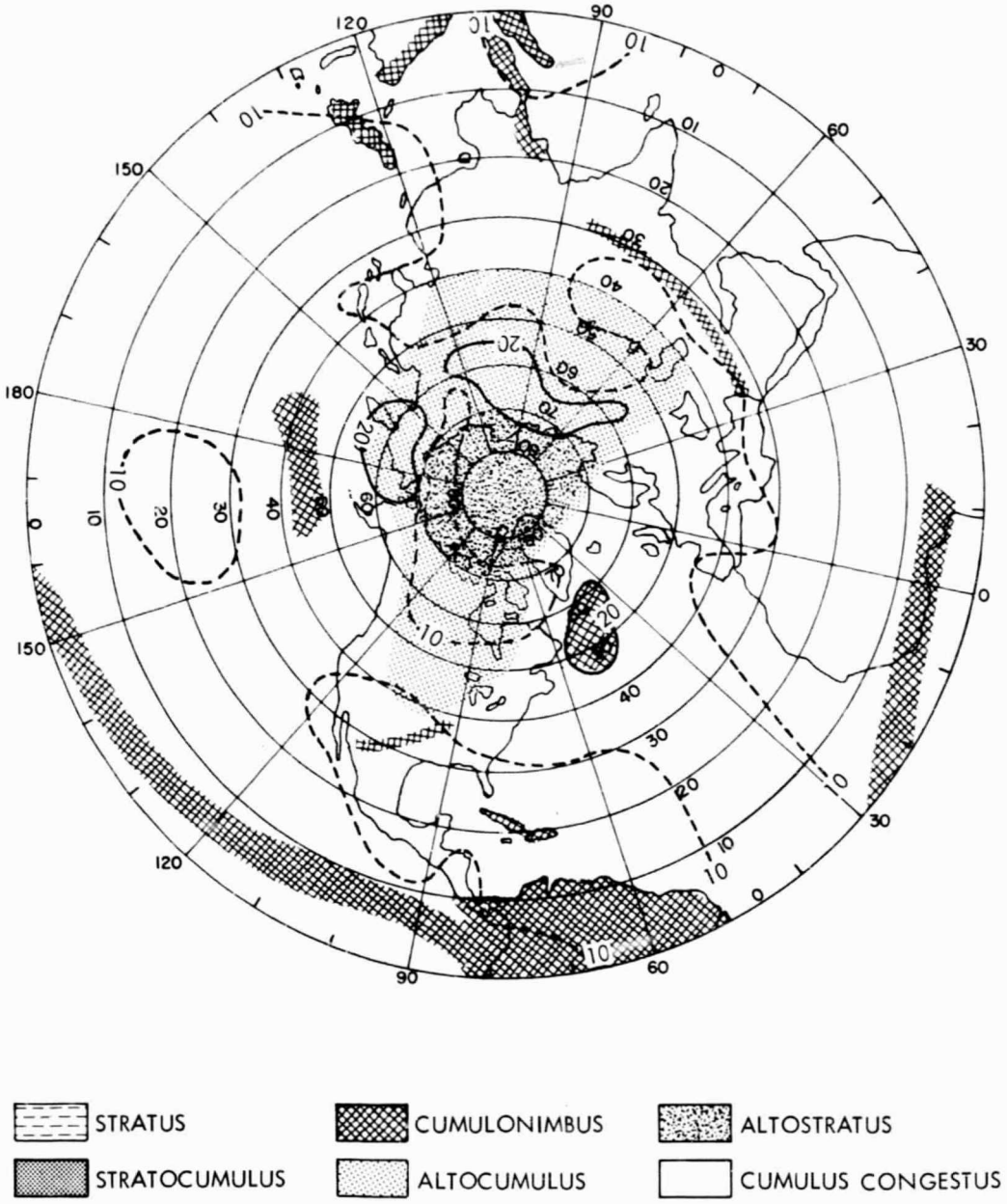

Figure A3--Percentage frequency of 6/10 to 10/10 cloud cover at altitudes from 10,000 to 15,000 feet (Winter).

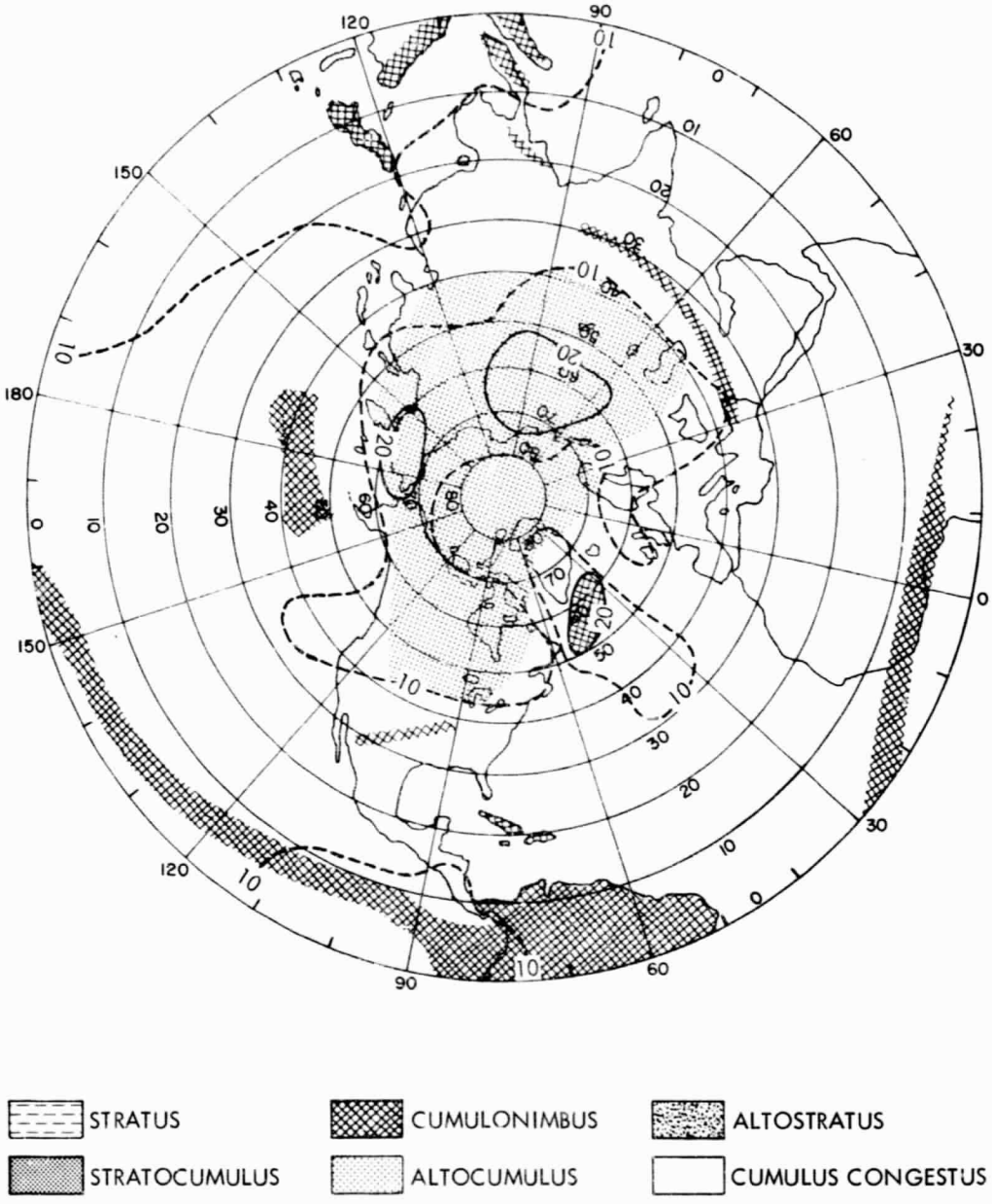

Figure A4—Percentage frequency of 6/10 to 10/10 cloud cover at altitudes from 15,000 to 20,000 feet (Winter).

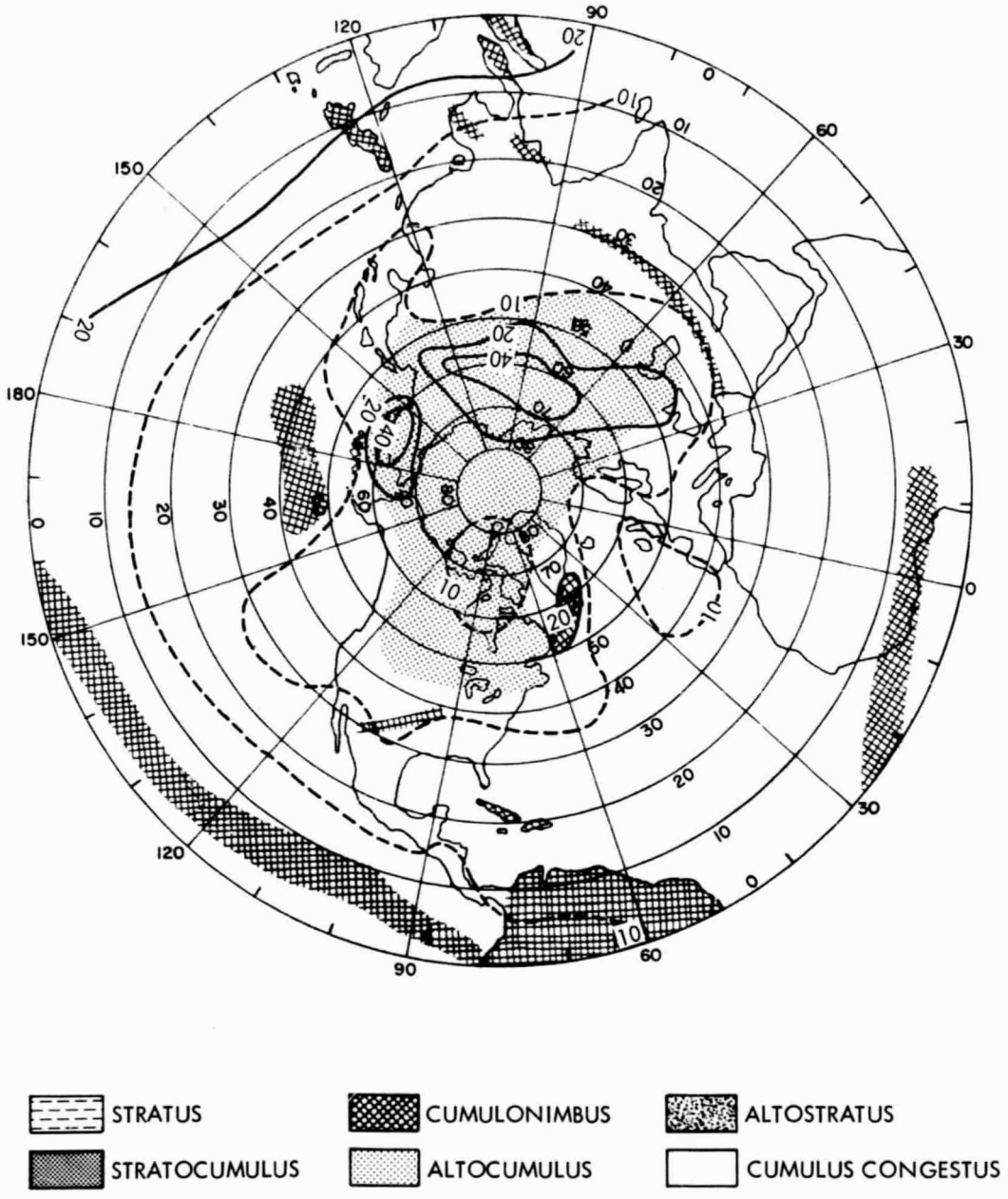

Figure A5—Percentage frequency of 6/10 to 10/10 cloud cover at altitudes from 20,000 to 30,000 feet (Winter).

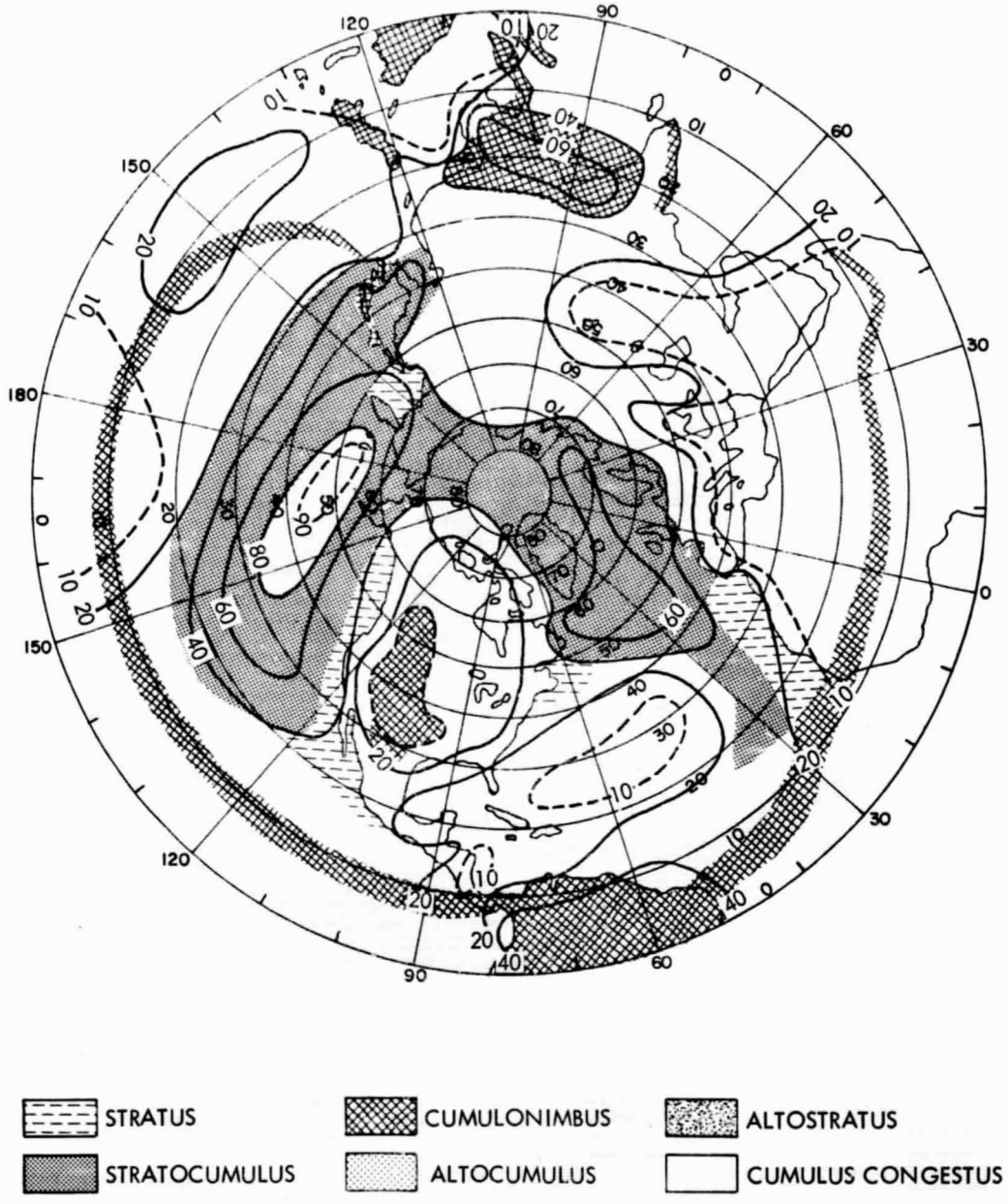

Figure A6—Percentage frequency of 6/10 to 10/10 cloud cover at altitudes from sea level to 5,000 feet (Summer).

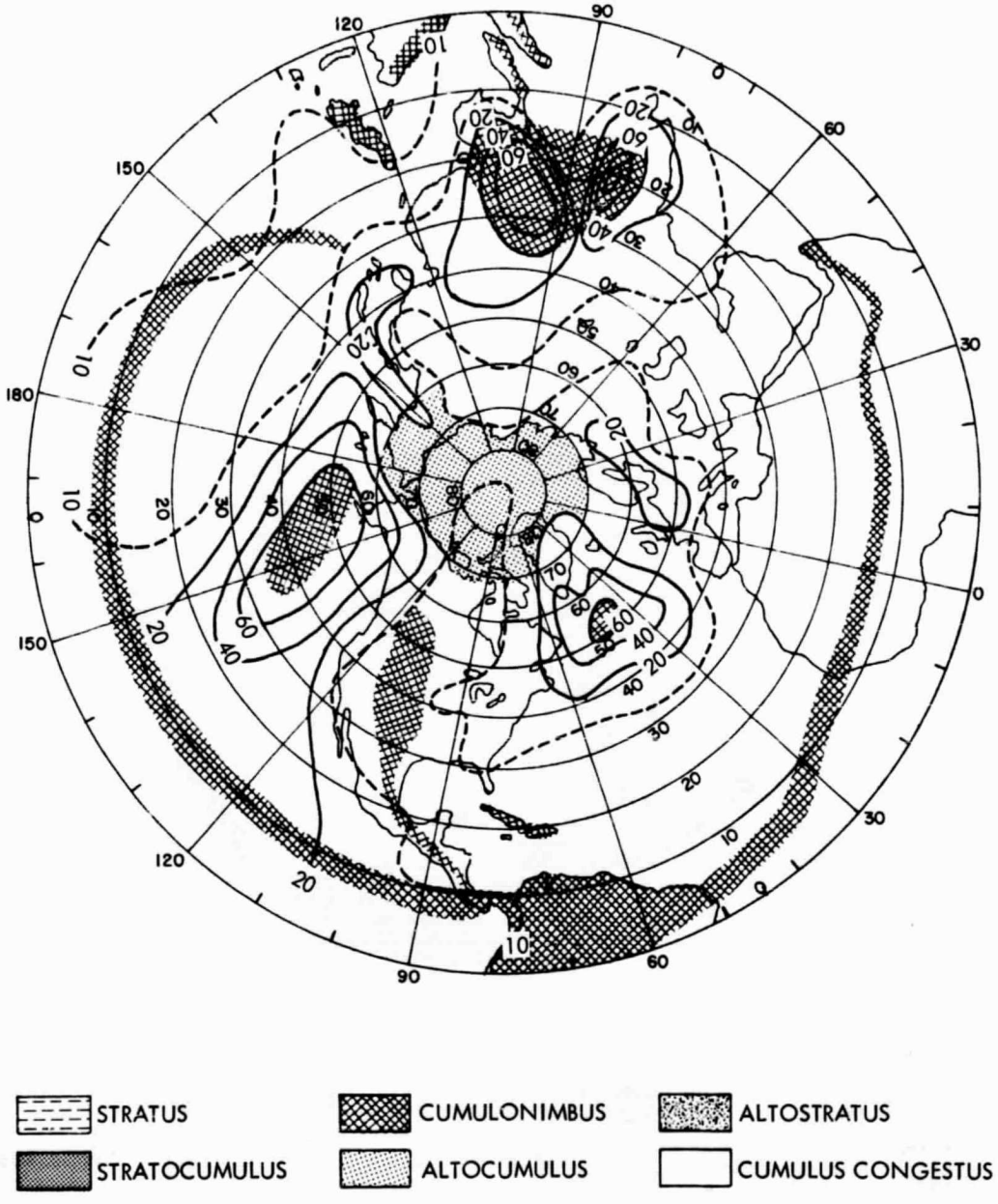

Figure A7—Percentage frequency of 6/10 to 10/10 cloud cover at altitudes from 5,000 to 10,000 feet (Summer).

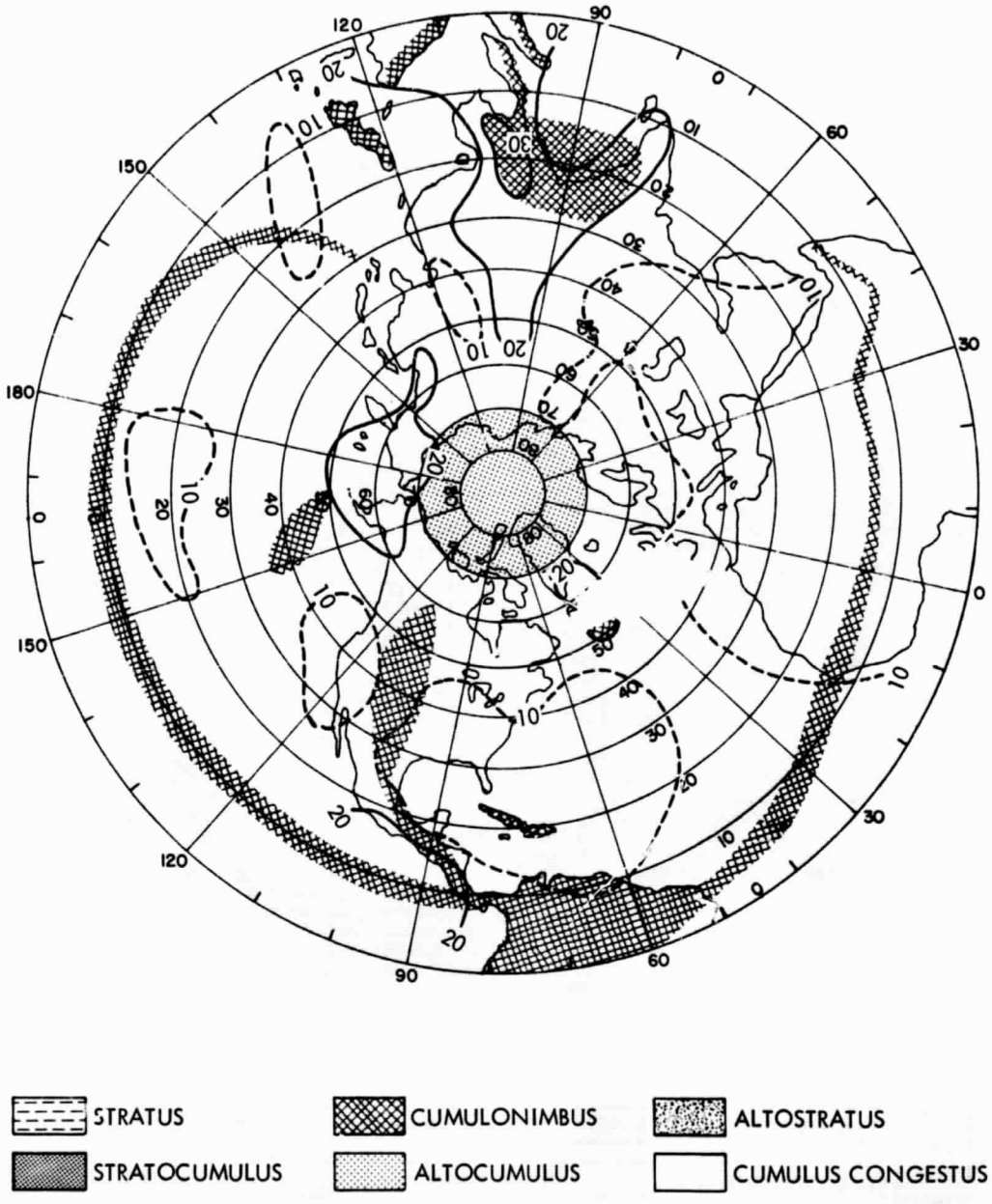

Figure A8—Percentage frequency of 6/10 to 10/10 cloud cover at altitudes from 10,000 to 15,000 feet (Summer).

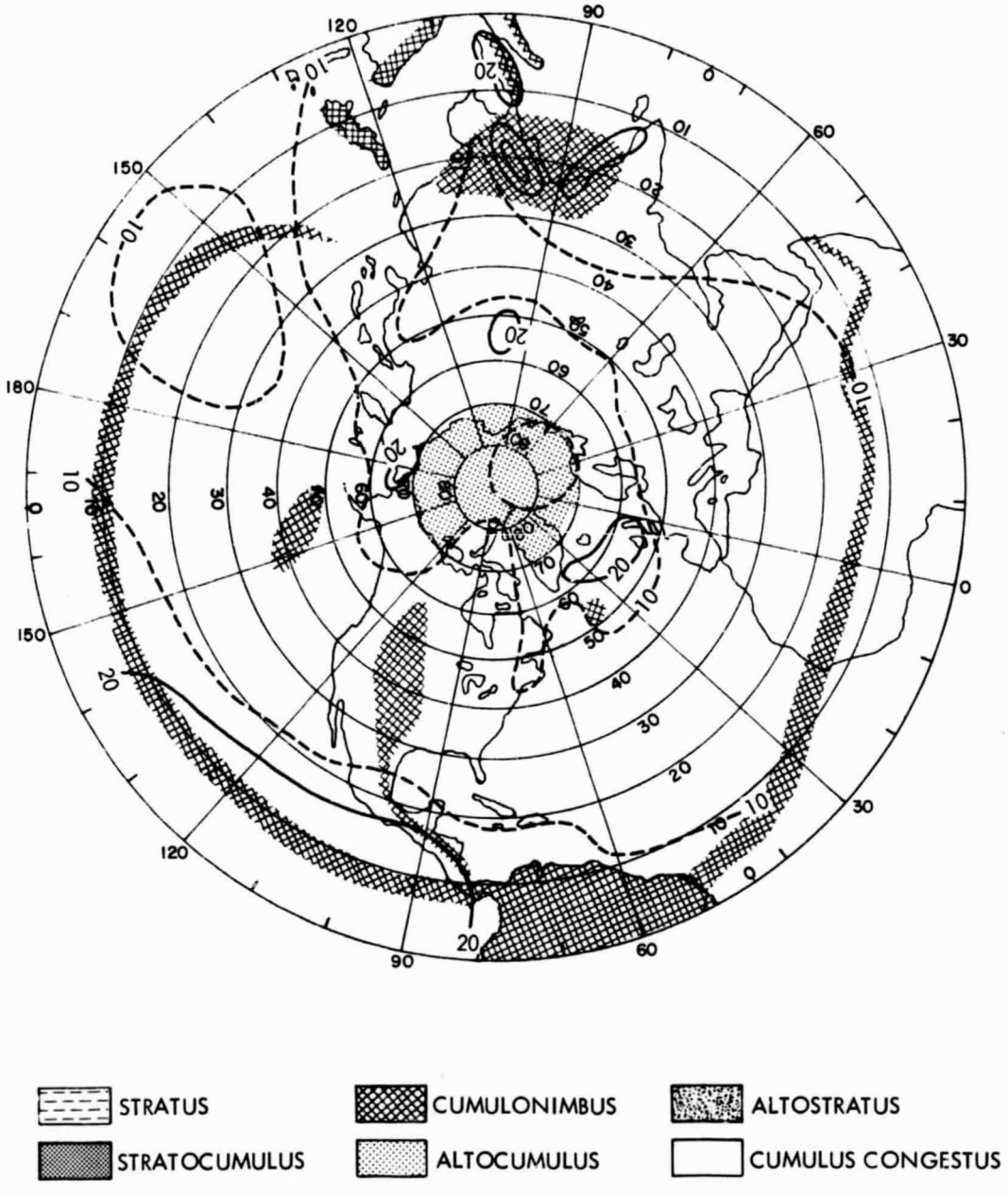

Figure A9—Percentage frequency of 6/10 to 10/10 cloud cover at altitudes from 15,000 to 20,000 feet (Summer).

APPENDIX B

POWER BUDGETS FOR ADVANCED LASER EXPERIMENTS

1.0 Introduction

The following paragraphs present preliminary uplink and downlink power budgets for the proposed 1.06 micron (μ) and 0.53μ laser experiments between a three-axis stabilized synchronous satellite and special earth stations. These budgets are illustrative in nature, and although believed accurate, a more detailed study would be required to accurately forecast expected system performance.

The following laser power budgets are realistic in the sense that they represent application of state-of-the-art laser power levels and optical systems. The laser retroreflector experiment emplanted on the moon by the Apollo 11 astronauts represents advanced state-of-the-art laser power levels and pulse widths together with the use of the 120-inch Lick telescope.

2.0 1.06μ Uplink

2.0.1 Link description

The 1.06μ uplink is envisioned as follows:

Wavelength — 1.06 micron (near-infrared) = 1064.1 nanometer (nm).

Transmitter — PCM modulated multi-laser (Nd:YAG) transmitter using forward channeling optics (ellipsoidal mirror-walled tube with spindle-shaped mirror center stop) equivalent to 24"-diameter diffraction-limited optics. Beam divergence of 1×10^{-4} radian.

Receiver — Compound direct detection receiver with gaseous microchannel optical preamps feeding avalanche photo diode detectors. Segmented solar furnace-type receiver optics totaling 1 m^2 in 16 elements.

Modulation — PCM with flexible pulse structure; pulse rate $\approx 10^2$ pulses per second (pps), pulse width $\approx$10-20 ns.

2.0.2 Uplink power budget

The symbols and quantities of interest to this 1.06μ uplink power budget are given in Table B-1. The following discussion will derive an expression for the false alarm- and error probabilities as

Table B-1

List of Quantities for the 1.06μ Uplink Receiver.

Symbol	Description
A_R	Effective area of receiving aperture in m^2
c	Velocity of light, 3×10^8 m/sec
f_R	Transmission factor of receiving aperture
f_F	Transmission factor of interference filter
G	Gain of one-way laser system
h	Planck's constant, 6.62×10^{-34} joule-sec
I	Radiant intensity of laser transmitter in photon/sec/ster
N_{SBS}	Receiver input noise due to solar backscatter from atmosphere in number of photons
N_{SR}	Receiver input noise due to solar backscatter from earth's surface in number of photons
N_{BBR}	Receiver input noise, due to blackbody radiation from the earth, incident in number of photons
N_n	$N_{SBS} + N_{SR} + N_{BBR}$
N_{DC}	Equivalent receiver input noise power due to dark current effects in photon/sec
P_N	Sum of P_{NA}, P_{NE}, P_{ND} in photon/sec
P_R	Received signal power in photon/sec
P_T	Transmitted power in photon/sec
R	Transmission path length, 3.6×10^7 meters
$\bar{R}$	Effective thickness of atmosphere in km
W_R	Signal radiant flux density at receiver in photon/sec - m^2
α	Reflective efficiency
Γ_A	Atmospheric backscatter anisotropy parameter, $1/8\pi$
δ	One-way path transmission factor, 0.25 at 1060 nanometer for 30° elevation (Reference B2)
λ	Wavelength of light in meters or nanometers (nm)
$\Delta\lambda$	Optical filter bandwidth in nm
θ_R	Receiver beamwidth in radians
θ_T	Transmitter beamwidth in radians, 1×10^{-4} radians
η	Optical frequency in hertz
ρ	Earth's effective reflectivity at vertical incidence
σ	Extinction coefficient
T	Transmitted pulse width in seconds (20 ns)

a function of various system parameters. In order to do this, the number of incident signal- and noise photons during a pulse interval at the front surface of the optical preamp must be determined.

The earth-based laser transmitter radiates a power of P_T photons per second uniformly in a narrow beamwidth of θ_T radians. In terms of solid angle, the radiant intensity of the transmitter is

$$I = \frac{4 P_T}{\pi \theta_T^2} \text{ photon/sec/steradian} . \tag{1}$$

The target is a satellite-borne receiver at a distance of R meters from the transmitter. The path medium causes attenuation of the signal; this factor is δ, the one-way path transmission loss. The radiant intensity at the receiver is then

$$W_R = \left[\frac{4 P_T}{\pi \theta_T^2}\right]\left[\frac{\delta}{R^2}\right] \text{ photon/sec/m}^2 . \tag{2}$$

Each lens in the segmented receiver optics has an area A_R, a transmission factor f_R, and reflective efficiency α. The interference filter has a transmission factor f_F. The received power is then

$$P_R = W_R A_R f_R \alpha f_F , \tag{3}$$

$$= \left[\frac{4 P_T}{\pi \theta_T^2}\right]\left[\frac{\delta}{R^2}\right]\left[A_R f_R \alpha f_F\right] \text{ watts} . \tag{4}$$

The energy per photon is

$$E_P = \frac{hc}{\lambda} , \tag{5}$$

so the number of photons of wavelength λ received during a transmitter pulse period T_s is

$$N_R = \frac{P_R T_s^{\lambda}}{hc} ; \tag{6}$$

$$N_R = \left[\frac{4 P_T}{\pi \theta_T^2}\right]\left[\frac{\delta}{R^2}\right]\left[A_R f_R \alpha f_F\right]\left[\frac{T_s^{\lambda}}{hc}\right] \text{ photons} . \tag{7}$$

Noise

The noise incident on the front surface of the gaseous microchannel optical preamplifier consists of four components: (1) backscattered solar radiation from the atmosphere, (2) reflected solar radiation from the earth's surface, (3) blackbody radiation of the earth, and (4) an equivalent incident noise flux due to dark-current effects in the optical preamp. These sources will now be treated one at a time. The noise terms are assumed here to be additive, although in practice they may be multiplicative in nature.

Backscattered Solar Radiation

The number of received photons due to solar backscatter from the atmosphere can be expressed (Reference B1) as

$$N_{SBS} = I_S(\theta, \lambda)\left[A_R f_R \alpha f_F(\Delta\lambda)\right]\left[\frac{\pi\theta_R^2}{4}\right]\left[\Gamma_A\left(1 - e^{-2\bar{R}\sigma}\right)\right]\left[\frac{T_g\lambda}{hc}\right]\left[\frac{1}{4\pi}\right] \quad (8)$$

where

$\Delta\lambda$ is the optical interference filter bandwidth,

θ_R is the beamwidth of the individual receiver in the segmented satellite optics,

$I_S(\theta, \lambda)$ is the solar spectral irradiance in watts/m^2-nm,

Γ_A is the atmospheric anisotropy coefficient = $1/8\pi$,

$\bar{R}$ is the effective thickness of the atmosphere,

σ is the atmospheric extinction coefficient.

Reflected Solar Radiation

The number of received photons due to solar reflection from the earth's surface is given (Reference B1) by

$$N_{SR} = I_S(\theta, \lambda)\left[A_R f_R \alpha f_F(\Delta\lambda)\right]\left[\frac{\pi\theta_R^2}{4}\right]\left[\rho e^{-2\bar{R}\sigma}\right]\left[\frac{T_g\lambda}{hc}\right]\left[\frac{1}{2\pi}\right] \quad (9)$$

where ρ is the effective reflectance of light from the earth at vertical incidence.

Blackbody Radiation

The spectral radiant emittance, W_λ, of a blackbody at temperature T is given (Reference B2) by

$$W_\lambda = \frac{C_1}{\lambda^5}\left[e^{(C_2/\lambda T)} - 1\right]^{-1} \text{ W/M}^2\text{-nm} , \tag{10}$$

where

$$C_1 = 3.74 \times 10^{21} \text{ W-nm}^4/\text{M}^2 ,$$

$$C_2 = 1.438 \times 10^7 \text{ nm-°K} .$$

Hence the number of photons due to blackbody radiation from the earth incident on the gaseous microchannel amplifier can be stated as

$$N_{BBR} = W_\lambda \left[A_R f_R \alpha f_F(\Delta\lambda)\right]\left[\pi\theta_R^2\right]\left[e^{-\bar{R}\sigma}\right]\left[\frac{T_s \lambda}{hc}\right]\left[\frac{1}{2\pi}\right] . \tag{11}$$

The contribution of the preceding three sources of noise can be expressed as

$$N_n = \left[I_s(\theta, \lambda)\left\{\frac{\Gamma_A\left(1 - e^{-\bar{R}\sigma}\right)}{2} + \rho e^{-2\bar{R}\sigma}\right\} + W_\lambda e^{-\bar{R}\sigma}\right]\left[A_R f_R \alpha f_F(\Delta\lambda)\right] \cdot \left[\frac{\pi\theta_R^2}{4}\right]\left[\frac{T_s \lambda}{hc}\right]\left[\frac{1}{2\pi}\right] . \tag{12}$$

Equivalent Dark-Current Photon Input

The gaseous microchannel optical preamplifier will possess a finite quiesent output in the absence of an input light flux. This extraneous output is the dark count, similar to dark-current effects in conventional photomultiplier tubes. In the absence of test data, dark-count characteristics are assumed to be the same as for standard photomultiplier tubes (Reference B3). An equivalent photon input flux to account for the dark-count is estimated to be $N_{DC} = 4 \times 10^8$ photons/sec at 1060 nm.

Total Input Noise

The total input noise at the front surface of the gaseous microchannel optical preamplifier is then the sum of the equivalent dark-count input with (12). To estimate the total number of incident noise photons, the following assumptions are made for the quantities involved:

$I_s(\theta, \lambda) \cong I_s(0°, 1060 \text{ nm}) \cong 7 \times 10^{-1}$ W/m²-nm (Reference B2)

$W_\lambda << 10^{-3}$ W/m²-nm (Reference B2)

$\bar{R}$ = 1.5 km (Reference B1)

ρ = 0.5 (approximated from Reference B4)

$\sigma \cong 0.1\ km^{-1}$ (Reference B4)

A_R = 1/16 m^2 (assuming a 4 × 4 receiving matrix totaling 1 m^2)

f_R = 0.9 (estimated)

T_S = 20 ns (estimated)

α = 0.95 (estimated)

f_F = 0.9 (estimated)

$\Delta\lambda$ = 1 nm (10 Å) (estimated)

$\theta_R = 10^{-3}$ radians (estimated)

Therefore the incident equivalent photon noise flux, neglecting blackbody radiation (i.e., $W_\lambda << I_S$), is given by (12). The various contributions to this noise flux during one 20-ns transmitter pulse width T_S are:

Backscattered solar radiation	1.25 Photons
Reflected solar radiation	166.40 Photons
Equivalent dark count	8.00 Photons
m = Total $\cong$	175.65 Photons.

It should be noted that dispersive refraction effects in the Earth's atmosphere will tend to delay or smear the received signal energy in time. These effects have been neglected here.

Required Transmitter Power

The required transmitter power can now be computed. The number of signal photons which reach the front surface of the gaseous microchannel amplifier is given by (7). This formula yields, as a function of P_T,

$$N_R = 1.26\, P_T \times 10^2 \text{ photons} . \tag{13}$$

The number of noise photons received in an interval T_S is assumed to fluctuate with Poisson statistics. That is, the probability of exactly K noise photons arriving in T_S seconds is given by

$$P_K = \frac{m^K}{K!} \exp(-m) , \tag{14}$$

where m is the average number of photons received during the interval T_S. For moderate m, (14) can be approximated by use of the Gaussian probability distribution, where

$$P(x) = \frac{1}{2\pi\sigma^2} \exp\left(\frac{-(x-m)^2}{2\sigma^2}\right) . \tag{15}$$

Therefore the probability that the number of noise photons received in an interval T_S will exceed some threshold value K_0 is just

$$P(K > K_0) = \int_{K_0}^{\infty} P(x)\, dx , \tag{16}$$

where σ^2 of $P(x)$ equals m of P_K.

Assuming a 1×10^{-6} error rate is required, together with a 1×10^{-6} probability of a false alarm, tables can be used to calculate K_0. For a false alarm probability of 1×10^{-6}, $K_0 \cong m + 4.75\sigma$, where $\sigma = (m)^{1/2} = (175.65)^{1/2}$. Also the transmitter power can be determined so that

$$1.26\, P_T \times 10^2 = m + 9.5\sigma , \tag{17}$$

or

$$P_T = \frac{m + 9.5\sigma}{1.26 \times 10^2} = 2.39 \text{ watts} . \tag{18}$$

This value of P_T is within the state-of-the-art. A threshold level corresponding to $K_0 = m + 4.75\sigma$ should be satisfactory for proper system operation under the constraints assumed.

3.0 0.53μ Uplink

3.0.1 Link description

The 0.53μ uplink is assumed to be equivalent to the 1.06μ uplink described in Section 2.0 but with a different operating wavelength.

3.0.2 Uplink power budget

Formulas (7) and (12) used in Paragraph 2.0.2 are also descriptive of the 0.53μ uplink. The equivalent dark-current photon input is estimated to be 9×10^6 photons/sec at 530 nm. Also,

$I_s(\theta, \lambda) = I_s(0°, 530 \text{ nm}) \cong 2 \text{ W/m}^2 \text{ - nm}$, (Reference B2)

$W_\lambda << 10^{-4}$ W/m²-nm, (Reference B2)

δ = 0.16 for a 30° elevation angle. (Reference B2)

All other quantities are assumed equal with the 1.06μ (1060 nm) case in Paragraph 2.0.2.

Total Input Noise

The total input noise at the front surface of the gaseous microchannel optical preamplifier is then the sum of the equivalent dark-count input with (12). Computing the various contributions to this noise flux during one 20-ns transmitter pulse width T_s gives for the 0.53μ uplink:

Backscattered Solar Radiation	1.78 photons
Reflected Solar Radiation	237.62 photons
Equivalent Dark Count	<1 photon
Total	$\approx$ 240 photons

Required Transmitter Power

The required transmitter power can now be computed in a manner similar to that used in Paragraph 2.0.2. The number of signal photons which reach the front surface of the gaseous microchannel optical preamplifier in T_s = 20 ns is computed from (7). This formula yields (at 0.53μ) as a function of P_T,

$$N_R = 40.38\, P_T \text{ photons} . \tag{19}$$

Utilizing Equation (16) with

$$\sigma^2 = m = 240$$

and again assuming a desired error rate/false alarm rate of 1×10^{-6}, the threshold K_0 should then equal $m + 4.75\sigma$. The transmitter power is then determined:

$$P_T = \frac{m + 9.5\sigma}{40.38} = 9.59 \text{ watts} . \tag{20}$$

This value of P_T is within the present state-of-the-art.

4.0 0.53μ Downlink

4.0.1 Link description

The 0.53μ downlink is envisioned as follows:

Wavelength — 0.53μ

Transmitter — Binary polarization modulated, frequency-doubled Nd:YAG transmitter laser, Q-switched and mode-locked, 7" diffraction limited Questar optics.

Receiver — Birefringent beam splitter, photomultiplier detector tubes, 24" diameter diffraction limited optics.

Modulation — Binary polarization modulation -RHCP, LHCP.

4.0.2 Downlink power budget

The various quantities of interest have already been discussed in Paragraph 2.0.2 and will not be repeated here. The principal sources of noise do change somewhat, however. Photomultiplier dark-current effects are present as are sky noise (day and night) and noise directly caused by such sources as the Sun, Moon, Venus, and Mars. Each noise source is treated separately in the following. Additivity is again assumed.

Dark-Current Effects

As discussed in Paragraph 2.0.2, both gaseous microchannel amplifiers and photomultiplier tubes have a quiescent output even with no incident light flux. It is estimated that an equivalent dark photon count of 7.6×10^6 photons/sec can be expected for the downlink photomultiplier.

Sky Noise

Sky noise (both day and night) is caused by Lambertian scattering and airglow effects. Since daylight operation is more severe, only Lambertian scattering of the solar illumination is discussed. The number of photons incident on the front surface of the photomultiplier tube in the ground-based receiver can be expressed as

$$N_{SN} = I_S(\theta, \lambda)\left[A_R f_R f_F f_P(\Delta\lambda)\right]\left[\frac{\pi\theta_R^2}{4}\right]\left[\Gamma_A\left(1 - e^{-\bar{k}\sigma}\right)\right]\left[\frac{T_e \lambda}{hc}\right]\left[\frac{1}{4\pi}\right], \tag{21}$$

where all quantities have been previously defined. This equation is identical with (8), except that the reflective efficiency α is omitted since no solar furnace reflectors are postulated in this downlink receiver. The additional factor f_P has been inserted to account for losses in the polarization separation optics and filters.

Other Noise Sources

It is assumed for the sake of simplicity that the Sun, Moon and Venus do not contribute to the received noise level.

Total Noise

Assuming that the only external noise contribution to the earth-based receiver is given by (21), the noise flux incident on each channel of the polarization modulation detection receiver is just half this amount. This is the case since the noise input flux is assumed to consist of equal parts of right- and left-hand polarized light. The equivalent input noise flux N_{DC} due to dark-current effects in the photomultiplier detectors is assumed to equal 9×10^6 photons/sec at 530 nm. Therefore the total equivalent noise flux incident on the photomultiplier detectors during a transmitter pulse interval is given by:

$$N_N = \frac{N_{SN}}{2} + N_{DC} T_s \cdot \tag{22}$$

N_{SN} can now be calculated using the following quantities:

$I_S (\theta, \lambda) = I_S (0°, 530 \text{ nm}) = 2 \text{ W/m}^2\text{-nm}$ (Reference B2),

$A_R = 0.292 \text{ m}^2$ (assuming 24-inch diameter optics),

$f_R = 0.9$ (estimated),

$f_F = 0.9$ (estimated),

$f_P = 0.6$ (estimated),

$\Delta\lambda = 1 \text{ nm}$ (10°A) (estimated),

$\theta_R = 2.2 \times 10^{-3}$ radian (estimated),

$\Gamma_A = 1/8\pi$,

$\bar{R} = 3.0 \text{ km}$ (Reference 1) (air mass of two (2) at 30° elevation),

$\sigma \tilde{=} 0.1 \text{ km}^{-1}$ (Reference B4),

$T_S = 20 \text{ ns}$ (estimated),

$\lambda = 530 \text{ nm}$,

$h = 6.62 \times 10^{-34}$ joules-sec,

$c = 3 \times 10^8$ m/sec.

Equation (21) yields for N_{SN} a value of 48 photons per time interval T_S. The total equivalent noise flux incident on the photomultiplier detector can be found. From Equation (22)

$$N_N = \frac{N_{SN}}{2} + N_{DC} T_S = 24 \text{ photons} . \tag{23}$$

Required Transmitter Power

The required satellite-based 0.53μ transmitter power output can now be found. Modifying Equation (7) for the downlink case, the number of signal photons incident on the photomultiplier in one transmitter pulse interval T_S is given by

$$N_R = \left[\frac{P_R T_S \lambda}{hc}\right] \text{ photons} , \tag{24}$$

$$= \left[\frac{4 P_T}{\pi \theta_T^2}\right]\left[\frac{\delta}{R^2}\right]\left[A_R f_R f_F f_P\right]\left[\frac{T_S \lambda}{hc}\right] \text{ photons} . \tag{25}$$

Substituting in Equation (25) for the various downlink factors previously mentioned in association with Equation (21) and setting

$\theta_T = 1 \times 10^{-5}$ radian (estimated for 7-inch optics),

$\delta = 0.16$ (corresponds to an air mass of two at an earth receiver elevation angle of 30 degrees from horizontal), (Reference 2) yields N_R in terms of P_T, or:

$$N_R = 1.19 \times 10^4 \times P_T \text{ photons} . \tag{26}$$

Now, utilizing Equation (26) with $\sigma^2 = m = 24$ and assuming a desired overall error rate/false alarm rate of 1×10^{-6} (5×10^{-7} per receiver channel), then the threshold K_0 should equal $m + 4.9\sigma$. The required transmitter power can now be found from Equation (26):

$$P_T = \frac{N_R}{1.19 \times 10^4} \text{ watts} , \tag{27}$$

$$P_T = \frac{m + 9.8\sigma}{1.19 \times 10^4} \text{ watts} , \tag{28}$$

or

$$P_T = 6.05 \times 10^{-3} \text{ watts} \tag{29}$$

at 530 nm.

5.0 1.06μ Downlink

5.0.1 Link description

The 1.06μ (1060 nm) downlink is envisioned to be similar to the 0.53μ downlink with the exception of operating wavelength. System details are given in Paragraph 4.0.1.

5.0.2 Downlink power budget

The various quantities of interest are developed in Paragraph 4.0.2 and are the same with the exception of wavelength-related terms.

Sky Noise

The sky noise (daytime) is also assumed to predominate in the 1.06μ (1060 nm) downlink receiver. Other sources of noise are neglected. Equation (21) can be used to calculate the sky noise photon count during a transmitter pulse period, substituting the following changes in quantities:

$I_S(\theta, \lambda) = I_S$ (0°,1060 nm) $\cong 7 \times 10^{-1}$ W/m^2 - nm. (Reference 2)

$\lambda = 1060$ nm.

Thus

$$N_{SN} \cong 34 \text{ photons} . \tag{30}$$

Total Noise

The total noise photon count per receiver channel per transmitter pulse period can be found from Equation (22):

$$N = \frac{N_{SN}}{2} + N_{DC} T_S \cong 17 \text{ photons} . \tag{31}$$

Required Transmitter Power

The required transmitter power can be determined from Equation (25). All factors are identical with the 0.53μ (530 nm) downlink case, except that λ is set to 1.06μ (1060 nm) and δ is 0.25 (air mass of two). Thus,

$$N_R = 3.72 \times 10^4 \times P_T \text{ photons} , \tag{32}$$

or

$$P'_T = \frac{N_B}{3.72 \times 10^4} . \tag{33}$$

Now proceeding in the same manner as before,

$$P_T = \frac{m + 9.8\sigma}{3.72 \times 10^4} , \tag{34}$$

where

$$\sigma^2 = m = 17 . \tag{35}$$

Thus

$$P_T = \frac{57.47}{3.72 \times 10^4} = 15.4 \times 10^{-4} = 1.54 \times 10^{-3} \text{ watts} \tag{36}$$

at 1060 nm.

6.0 Cubecorner Reflectors

6.0.1 System description

This particular link budget considers the use of earth-based laser transmitter and receiver with cubecorner retro-reflectors on board the spacecraft. The spacecraft is in a synchronous equatorial orbit.

6.0.2 Laser system description

Two wavelengths of operation are considered: 1.06μ (1060 nm) and 0.53μ (530 nm). This coincides with the previously discussed up- and downlink power budgets in Paragraphs 2, 3, 4 and 5.

The earth-based transmitter is similar to that discussed in Paragraph 2.0.1. The earth-based receiver is similar to that discussed in Paragraph 4.0.1 with the exception that straightforward pulse modulation is used, which requires only a direct detection receiver using photomultiplier tubes.

6.0.3 Power budget

The target on the spacecraft consists of a panel of cubecorner reflectors whose area is A_s and whose reflective efficiency is E_c. These reflectors return incident radiation in a narrow beam along

its path of incidence. From Equation (2), the reflected power from the panel is:

$$P_A = [P_T A_S E_C]\left[\frac{4}{\pi\theta_T^2}\right]\left[\frac{\delta}{R^2}\right] \text{ watts} . \tag{37}$$

This power is reflected into a beam of θ_S radians. Therefore, the radiant intensity of the cubecorner reflector panel is:

$$I_S = [P_T A_S E_C]\left[\frac{4}{\pi\theta_T^2}\right]\left[\frac{4}{\pi\theta_S^2}\right]\left[\frac{\delta}{R^2}\right]\left[\frac{\lambda}{hc}\right] \text{ photons/sec ster} . \tag{38}$$

Since the reflected energy travels the same path in the downlink as it did in the uplink, the radiant flux density at the receiver is given by:

$$W_R = [P_T A_S E_C]\left[\frac{4}{\pi\theta_T^2}\right]\left[\frac{4}{\pi\theta_S^2}\right]\left[\frac{\delta^2}{R^4}\right]\left[\frac{\lambda}{hc}\right] . \tag{39}$$

Therefore, the number of photons received at the photomultiplier input surface during one transmitter pulse period is given by:

$$N_R = [P_T A_S A_R f_R f_F E_C]\left[\frac{4}{\pi\theta_T^2}\right]\left[\frac{4}{\pi\theta_S^2}\right]\left[\frac{\delta^2}{R^4}\right]\left[\frac{T_S \lambda}{hc}\right] \text{ photons} . \tag{40}$$

Noise

Only sky noise is considered for the present case of satellite-borne laser cubecorner retroreflectors. Sky noise was discussed in Paragraph 4.0.2. Equation (21) is directly applicable here. Such noise sources as the Sun, Moon and Venus are assumed to be outside the receiver's field of view.

Since a single channel direct detection receiver is assumed, the total equivalent noise photon count can be stated as

$$N_N = N_{SN} + N_{DC} \cdot T_S . \tag{41}$$

or

$$N_N \cong 48 \text{ photons } (\lambda = 530 \text{ nm}) , \tag{42}$$

$$N_N \cong 34 \text{ photons } (\lambda = 1060 \text{ nm}) . \tag{43}$$

The same set of factors as used in Paragraphs 4.0.2 and 5.0.2 for noise calculations are assumed for the results given in Equations (42) and (43), respectively.

Required Transmitter Power

The required transmitter power can now be found by solving Equation (40) for P_T in terms of N_R and determining N_R for a false alarm/error rate of 1×10^{-6}. This procedure is identical with that first described in Paragraph 2.0.2.

The various factors used in Equation (40) are identical to those used in Paragraphs 4.0.2 and 5.0.2 for the 0.53μ (530 nm) and 1.06μ (1060 nm) downlink calculations. The newly introduced or modified quantities are as follows:

$A_s = 0.2$ m^2 (estimated),

$E_c = 0.3$ (estimated),

$\theta_T = 1 \times 10^{-4}$ radians (estimated),

$\theta_s = 4.8 \times 10^{-5}$ radians; 10 arc-seconds (estimated).

Thus, substituting the factors into Equation (40) yields:

$$P_T = \frac{N_R}{8.12 \times 10^{-7}} \text{ watts } (\lambda = 530 \text{ nm}) . \tag{44}$$

and

$$P_T = \frac{N_R}{3.97 \times 10^{-6}} \text{ watts } (\lambda = 1060 \text{ nm}) . \tag{45}$$

Following the development of preceding paragraphs the required N_R for proper single pulse detection at 1×10^{-6} error/false alarm rates, for

$$\lambda = 530 \text{ nm:}$$

$$K_0 = m + 4.75\,\sigma , \tag{46}$$

where

$$m = \sigma^2 = 48 , \tag{47}$$

so that

$$P_T = \frac{m + 9.5\sigma}{8.12 \times 10^{-7}} \text{ watts}, \tag{48}$$

$$\cong 1.40 \times 10^{8} \text{ watts } (\lambda = 530 \text{ nm}). \tag{49}$$

For λ = 1060 nm:

$$K_0 = m + 4.75\sigma, \tag{50}$$

where

$$m = \sigma^2 = 34, \tag{51}$$

so that

$$P_T = \frac{m + 9.5\sigma}{3.97 \times 10^{-6}} \text{ watts}, \tag{52}$$

$$= 2.26 \times 10^{7} \text{ watts } (\lambda = 1060 \text{ nm}). \tag{53}$$

Further study is required to determine the advisability of using laser retro-reflectors on synchronous altitude satellites for tracking purposes.

REFERENCES

B1. "Space Geodesy Altimetry Study," Raytheon Company, Space and Information Systems Division, Sudbury, Massachusetts. Final Report, NASA Contract NASW-1709, October 1968.

B2. Jensen, N., "Optical and Photographic Reconnaissance Systems," 1968. New York: John Wiley and Sons, Inc.

B3. "RCA Phototubes and Photocells," Radio Corporation of America, Lancaster, Pennsylvania. Technical Manual PT-60, 1963.

B4. Wolfe, W. L. (Ed), "Handbook of Military Infrared Technology," Office of Naval Research. Department of the Navy, Washington, D. C., 1965.